Electronic Supplementary Material (ESI) for RSC Advances.

Templating effect of 1,5-Disubstituted 1,2,3-Triazole-linked disaccharides on size, shape and antibacterial activity of silver nanoparticles

Anirban Kayet[a], Dhrubajyoti Datta[a], Ganesh Kumar[b], Anindya Sundar Ghosh[b]* and Tanmaya Pathak[a]*

[a]Department of Chemistry, Indian Institute of Technology Kharagpur, Kharagpur 721 302, India

[b]Department of Biotechnology, Indian Institute of Technology Kharagpur, Kharagpur 721302, India

Phone: +91-3222-283342; Fax: +91-3222-282252 (T. Pathak), +91-3222-283798 (A. S. Ghosh)

e.mail: tpathak@chem.iitkgp.ernet.in (T. Pathak); asghosh@ hijli.iitkgp.ernet.in (A. S. Ghosh)

List of contents:

Experimental Section:

General methods: Most of the reactions were conducted under nitrogen atmosphere. Melting points were determined in open-end capillary tubes and uncorrected. Carbohydrates and other fine chemicals were obtained from commercial suppliers and are used without purification. Solvents were dried and distilled following the standard procedures. TLC was carried out on pre-coated silica gel plates and the spots were visualized with UV light or by charring the plates dipped in 5% H_2SO_4-MeOH solution or in 5% H_2SO_4-vaniline-EtOH solution. Column chromatography was performed on silica gel (230-400 mesh). ^1H and ^{13}C NMR for compounds were recorded at 200/400/600 MHz instrument using $CDCl_3$, d_6-DMSO and D_2O as the solvent. DEPT experiments have been carried out to identify the methylene carbons. Optical rotations were recorded at 589 nm. High Resolution Mass Spectra (HRMS) were recorded by quadruple-equipped TOF mass spectrometer.

Synthesis of 1,5-disubstituted 1,2,3-triazole (1,5-DT) linked disaccharides 3 and 4:

A mixture of vinyl sulfone-modified carbohydrate **7**[1] or **8**[1] (1 equiv) and azidosugar **9**[2] (1.5 equiv) in water (5 mL/mmol) was heated under reflux for 36-40 h to afford 1,5-disubstituted 1,2,3-triazole linked disaccharides **10** and **11** (Scheme 1-ESI) using our recently reported strategies.[1,3] The 1,2-*O*-isopropyledene group of vinyl sulfone **7** or **8** and azidosugar **9** were unstable under the reaction condition due to the elimination of sulfinic acid during triazole formation and hence 1.5 equivalent of $NaHCO_3$ was added to the reaction mixture.

To a well-stirred solution of the mono-benzylated compounds **10** and **11** (1 equivalent) were added 10% Pd/C (2 equiv) and $HCOONH_4$ (7 equiv) in MeOH and the reaction mixtures were refluxed for 12 h. After completion of the reaction (TLC) the catalyst was filtered through celite

and the solvent was evaporated to dryness to give a residue. The residue was purified over silica gel column chromatography to afford the partially protected compounds **1** and **2** (Scheme 1-ESI).

The partially protected compounds **1** and **2** (1 equivalent) were dissolved in 70% TFA/DCM (2 mL/mmol) and the reaction mixtures were allowed to stire at room temperature for 48 h. After 48 h, the acids were removed under reduced pressure and the residues were washed with chilled ether to afford the fully deprotected compounds **3** and **4** (Scheme 1-ESI).

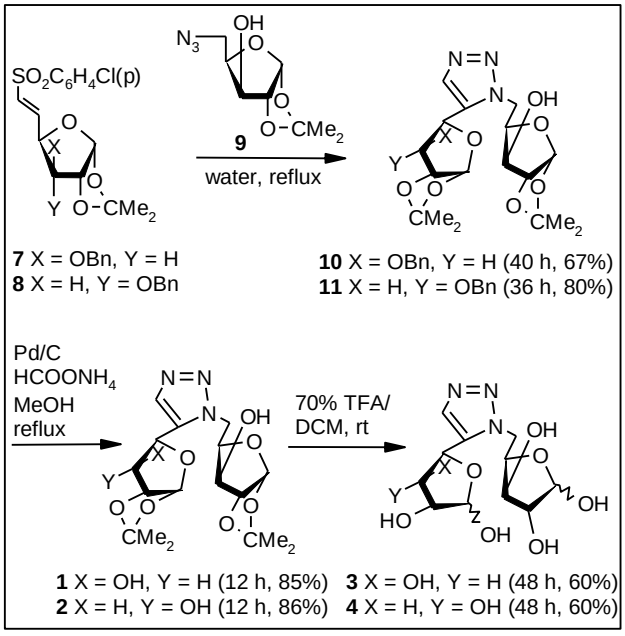

Scheme 1-ESI: Synthesis of 1,5-disubstituted 1,2,3-triazole-linked furanoside-furanoside dimmers.

After synthesizing the compounds 3 and 4, it was necessary to unambiguously establish the structures of these compounds. The structures of these compounds were confirmed from the x-ray analysis of the crystals of the benzylated derivatives of **1** and **2** (Figure 1-ESI).

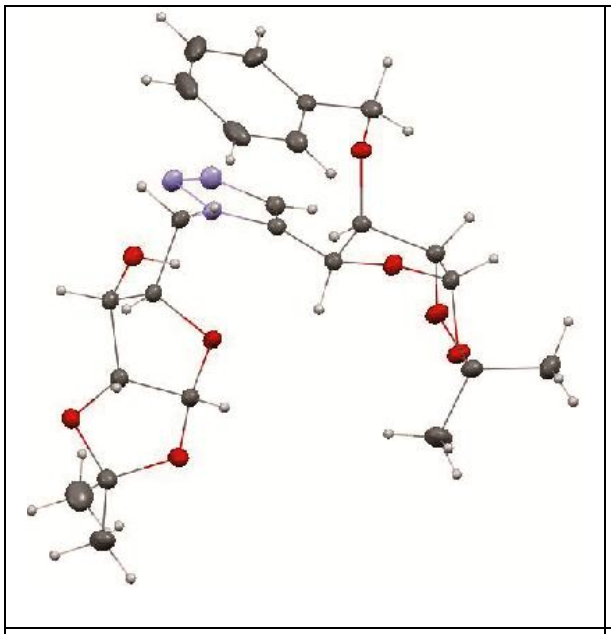

Crystal structure of compound **10**

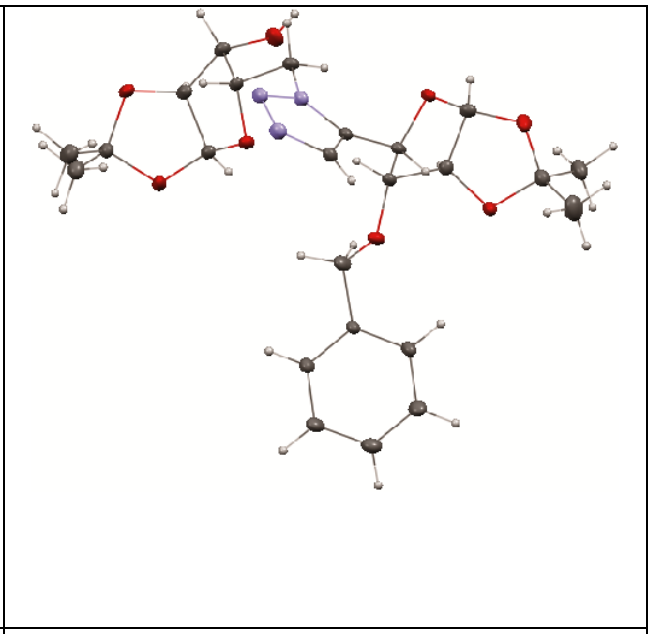

Crystal structure of compound **11**

Figure 1-ESI: Crystal structure of the 1,5-DT linked furanoside-furanoside dimers **10** and **11**.

Compound 10: Following the general procedure, over 40 h compound **7** (0.25 g, 0.55 mmol) was converted to **10** (0.18 g, 67 %). Eluent: EtOAc/petroleum ether (3:7). White solid. Mp. 108-110 ^{o}C; $[\alpha]^{25.2}_{D}$ = 52.4 (*c* 0.8, $CHCl_3$); ^{1}H NMR (200 MHz, $CDCl_3$): δ 1.24 (s, 3H), 1.31 (s, 3H), 1.36 (s, 3H), 1.48 (s, 3H), 4.00-4.05 (m, 2H), 4.26-4.52 (m, 7H), 4.68 (d, 1H, *J* = 3.6 Hz), 5.37 (d, 1H, *J* = 3Hz), 5.88 (d, 1H, *J* = 3.2 Hz), 6.03 (d, 1H, *J* = 3.4 Hz), 6.93-6.95 (m, 2H), 7.22-7.23 (m, 3H), 7.58 (s, 1H); ^{13}C NMR (50 MHz, $CDCl_3$): δ 26.3, 26.9, 46.9 (CH_2), 72.1 (CH_2), 73.9, 74.4, 79.5, 82.1, 82.4, 85.2, 104.9, 105.2, 112.0, 112.6, 128.0, 128.5, 128.8, 132.6, 133.9, 136.3; HRMS [ES^+, $(M+H)^+$]: for $C_{24}H_{32}N_3O_8$ found 490.2175, calcd 490.2189.

***Compound 11*:** Following the general procedure, over 36 h compound **8** (0.2 g, 0.44 mmol) was converted to **11** (0.17 g, 80%); Eluent: EtOAc/petroleum ether (3:7); White solid. Mp. 110-112 ^{o}C; $[\alpha]^{27}_{D}$ = 56.8 (*c* 0.6, $CHCl_3$); ^{1}H NMR (200 MHz, $CDCl_3$): δ 1.28 (s, 3H), 1.40 (s, 3H), 1.44

(s, 3H), 1.65 (s, 3H), 3.90 (dd, 1H, *J* = 4.1 Hz, 9.0 Hz), 4.03 (d, 1H, *J* = 2.6 Hz), 4.49-4.55 (m, 3H), 4.66-4.77 (m, 4H), 5.23 (d, 1H, *J* = 9.0 Hz), 5.90 (dd, 2H, *J* = 3.6 Hz, 13.0 Hz), 7.22-7.35 (m, 5H), 7.53 (s, 1H); ^{13}C NMR (50 MHz, $CDCl_3$): δ 26.3, 26.6, 26.9 (2 X C), 46.4 (CH_2), 70.3, 72.5 (CH_2), 74.8, 76.7, 79.4, 82.1, 85.1, 104.3, 105.2, 112.1, 113.8, 128.3, 128.6, 128.8, 132.3, 135.4, 136.4; HRMS [ES^+, $(M+H)^+$]: for $C_{24}H_{32}N_3O_8$ found 490.2199, calcd 490.2189.

Compound 1*:* Following the general procedure, over 12 h compound **10** (0.80 g, 1.38 mmol) was converted to the debenzylated compound **1** (0.47 g, 85%); Eluent: EtOAc/petroleum ether (4:1); White solid. mp. 187 ^{o}C; $[\alpha]^{27}_{D}$ = 54.4 (*c* 0.8, MeOH); ^{1}H NMR (400 MHz, D_2O): δ 1.42 (s, 3H), 1.49 (s, 3H), 1.53 (s, 3H), 1.66 (s, 3H), 4.41 (d, 1H, *J* = 1.6 Hz), 4.56 (d, 1H, *J* = 2.4 Hz), 4.67-4.75 (m, 2H), 4.93-4.98 (m, 2H), 5.67 (d, 1H, *J* = 2.4 Hz), 6.13 (d, 1H, *J* = 3.6 Hz), 6.27 (d, 1H, *J* = 4.0 Hz), 7.94 (s, 1H); ^{13}C NMR (50 MHz, D_2O): δ 25.7, 25.8, 26.2, 26.4, 48.6 (CH_2), 74.5, 74.8, 75.2, 80.0, 85.3, 104.8, 105.2, 113.3, 113.6, 134.0, 134.8; HRMS [ES^+, $(M+H)^+$]: for $C_{17}H_{26}N_3O_8$ found 400.1705, calcd 400.1720.

Compound 2: Following the general procedure, over 12 h compound **11** (0.80 g, 1.38 mmol) was converted to the debenzylated compound **2** (0.47 g, 86%); Eluent: EtOAc/petroleum ether (4:1); White solid. Mp. 170 ^{o}C; $[\alpha]^{27}_{D}$ = 42.8 (*c* 0.8, MeOH); ^{1}H NMR (200 MHz, d_6-DMSO): δ 1.17 (s, 3H), 1.27 (s, 6H), 1.47 (s, 3H), 3.98 (d, 2H, *J* = 8.8 Hz), 4.38-4.55 (m, 5H), 5.00 (d, 1H, *J* = 9.2 Hz), 5.62-5.82 (m, 3H), 7.67 (s, 1H); ^{13}C NMR (50 MHz, d_6-DMSO): δ 26.1, 26.5, 26.7, 26.8, 47.5 (CH_2), 71.1, 73.7, 76.0, 79.3, 79.5, 85.1, 103.5, 104.6, 110.9, 112.2, 131.9, 136.1; HRMS [ES^+, $(M+H)^+$]: for $C_{17}H_{26}N_3O_8$ found 400.1715, calcd 400.1720.

Compound 3: Following the general procedure, over 48 h compound **1** (0.50 g, 1.25 mmol) was converted to compound **3** (0.24 g, 60%) as brown solid. Mp. Charred at 60 ^{o}C; $[\alpha]^{27}_{D}$ = 62.4 (*c* 0.8, MeOH); ^{1}H NMR (200 MHz, D_2O): δ 4.11-4.80 (m, 14H), 4.99-6.12 (m, 3H), 8.13 (s, 1H); ^{13}C NMR (50 MHz, D_2O): δ 48.5 (CH_2), 74.4, 74.7, 75.1, 79.9, 85.2, 104.8, 105.1, 133.9, 134.7; HRMS [ES^+, $(M+H)^+$]: for $C_{11}H_{18}N_3O_8$ found 320.1123, calcd 320.1094.

Compound 4*:* Following the general procedure, over 48 h compound **2** (0.35 g, 0.88 mmol) was converted to compound **4** (0.17 g, 60%) as brownish solid. Mp. Charred at (60-62) ^{o}C; $[\alpha]^{27}_{D}$ = 72.2 (*c* 0.8, MeOH); ^{1}H NMR (200 MHz, D_2O): δ 4.10-4.68 (m, 12H), 5.18-5.73 (m, 3H), 8.17 (s, 1H); ^{13}C NMR (50 MHz, D_2O): δ 47.6 (CH_2), 71.2, 73.8, 76.1, 79.4, 79.6, 85.2, 103.7, 104.7, 132.0, 136.2; HRMS [ES^+, $(M+H)^+$]: for $C_{11}H_{18}N_3O_8$ found 320.1100, calcd 320.1094.

^{1}H NMR spectrum of 10

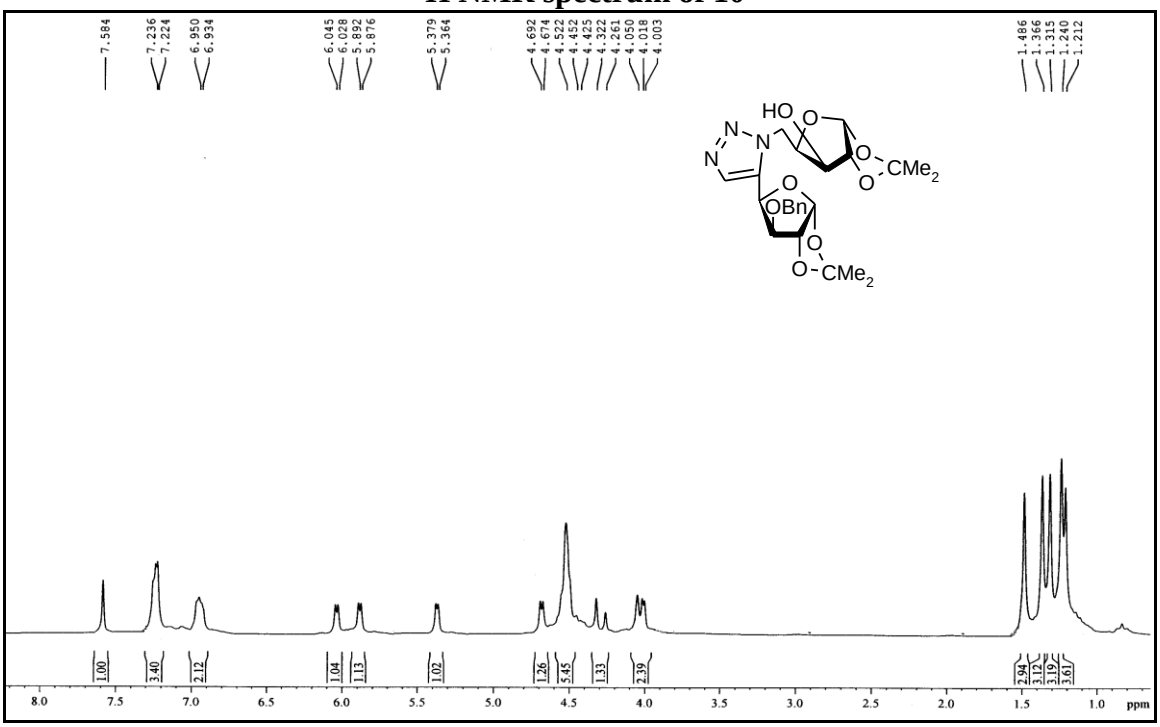

^{13}C NMR spectrum of 10

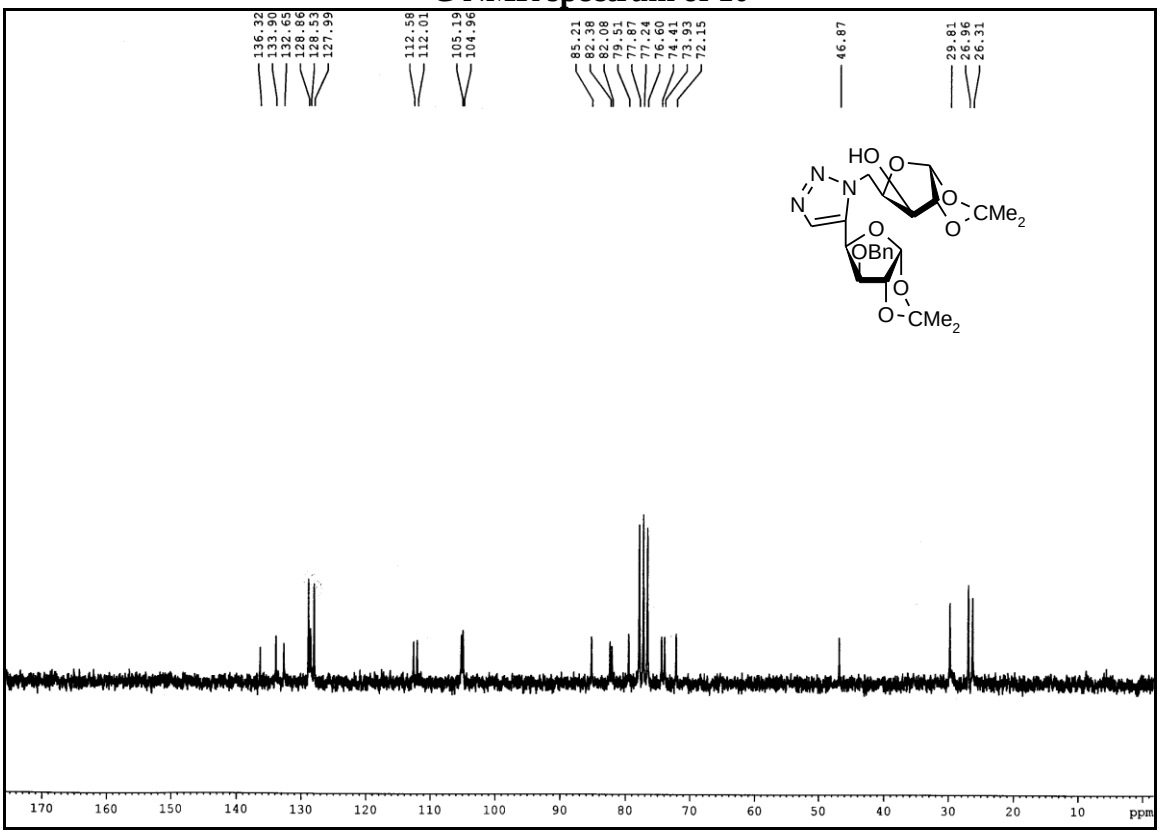

DEPT spectrum of 10

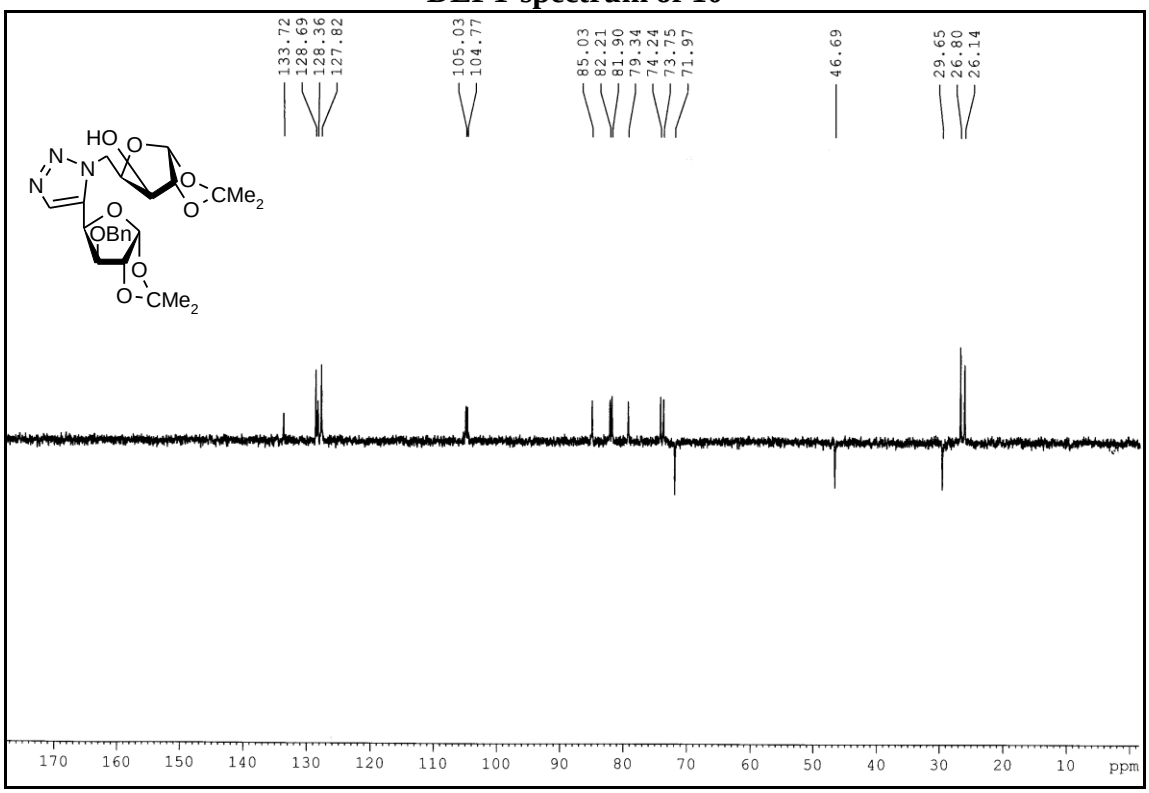

^{1}H NMR spectrum of 11

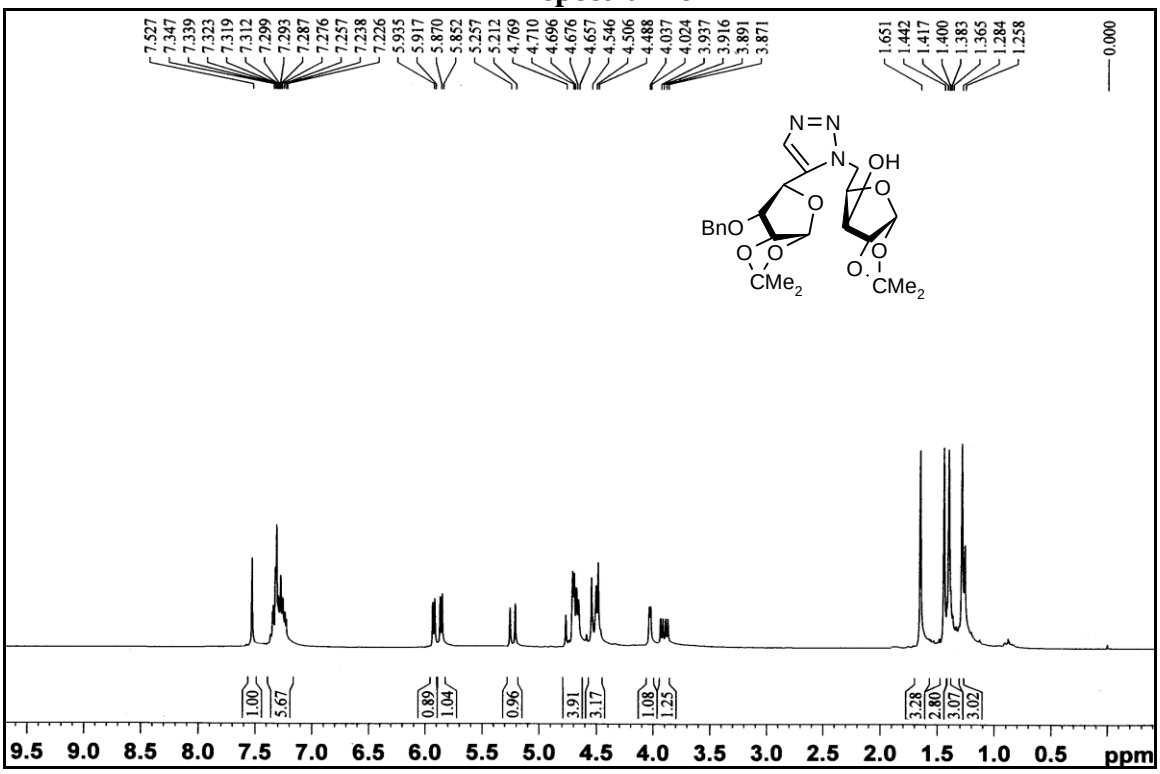

^{13}C NMR spectrum of 11

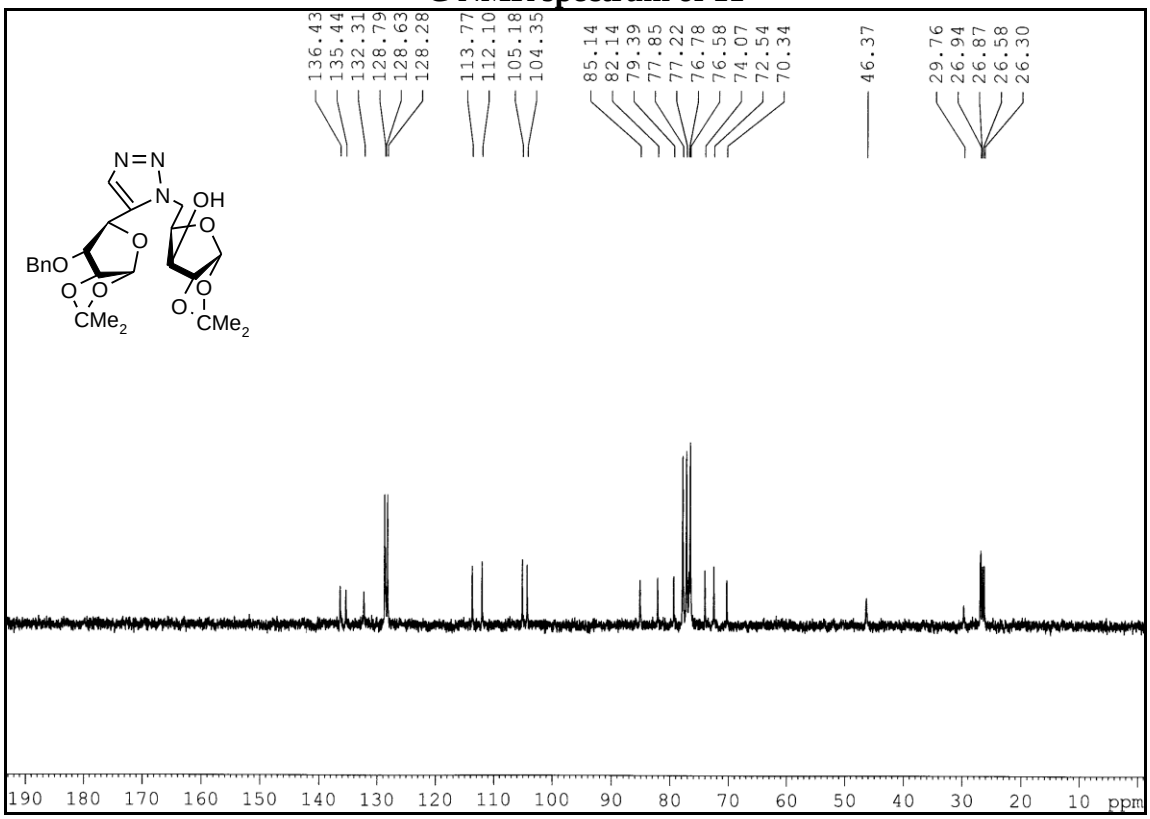

DEPT spectrum of 11

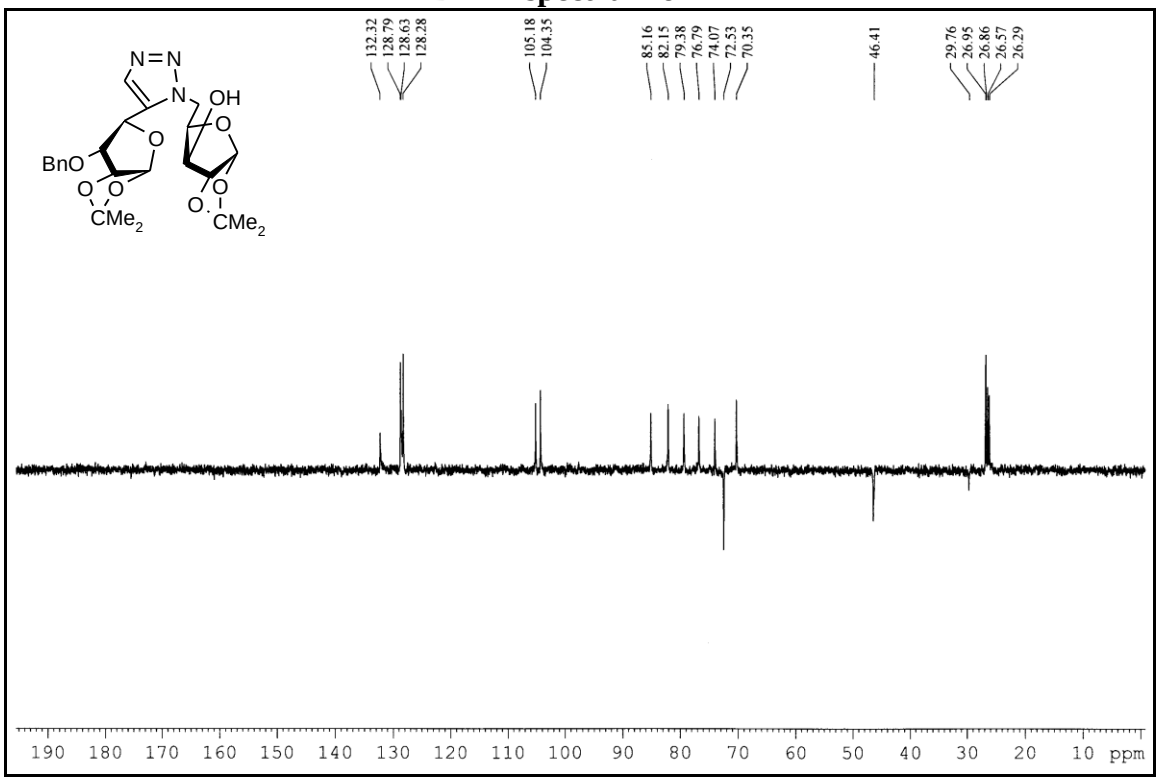

^{1}H NMR spectrum of 1

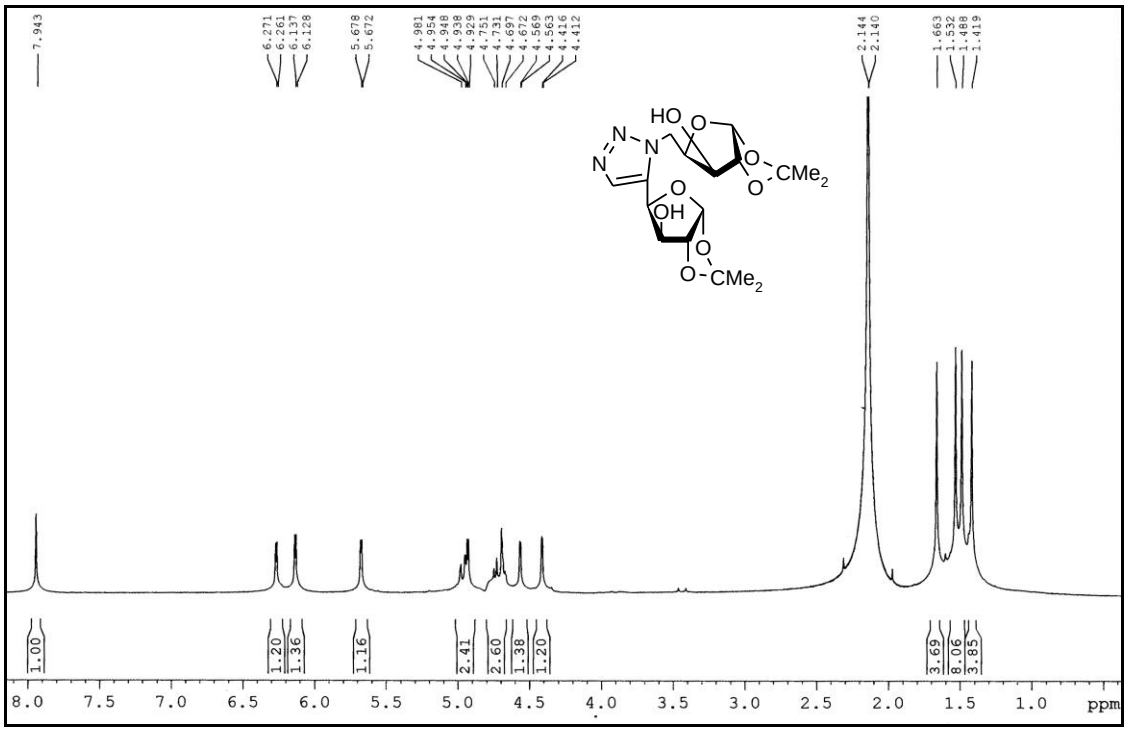

^{13}C NMR spectrum of 1

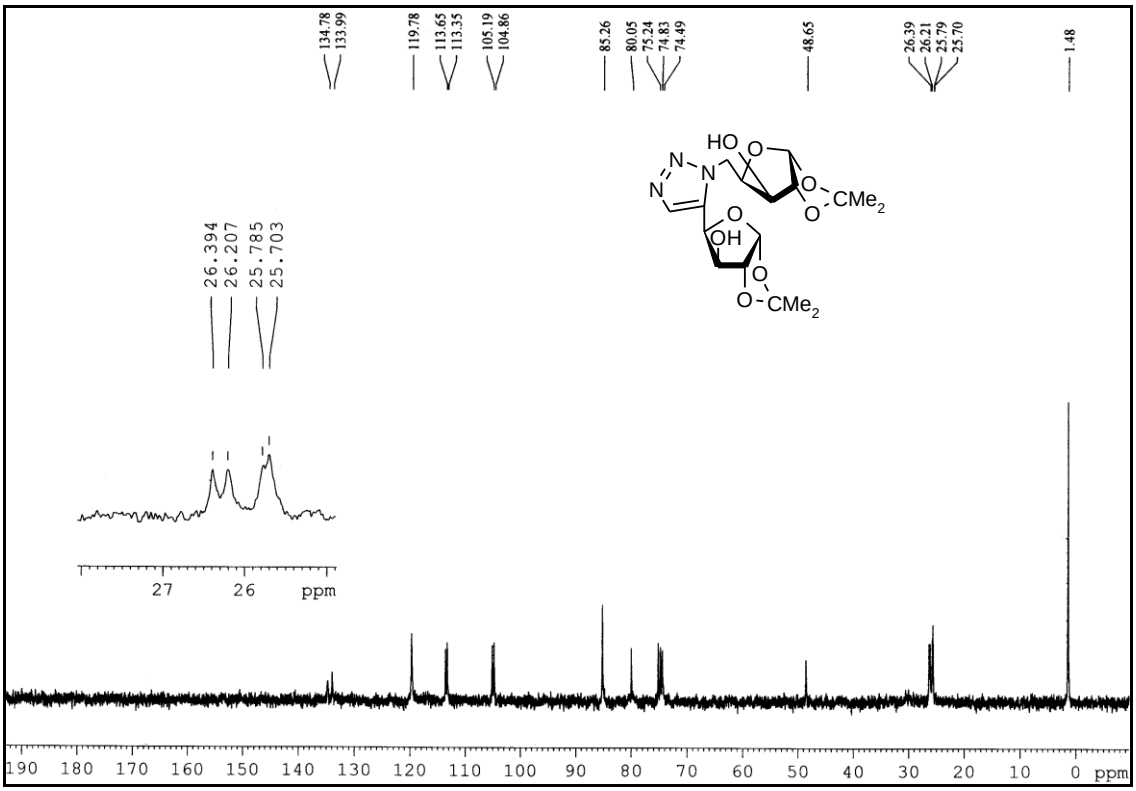

DEPT spectrum of 1

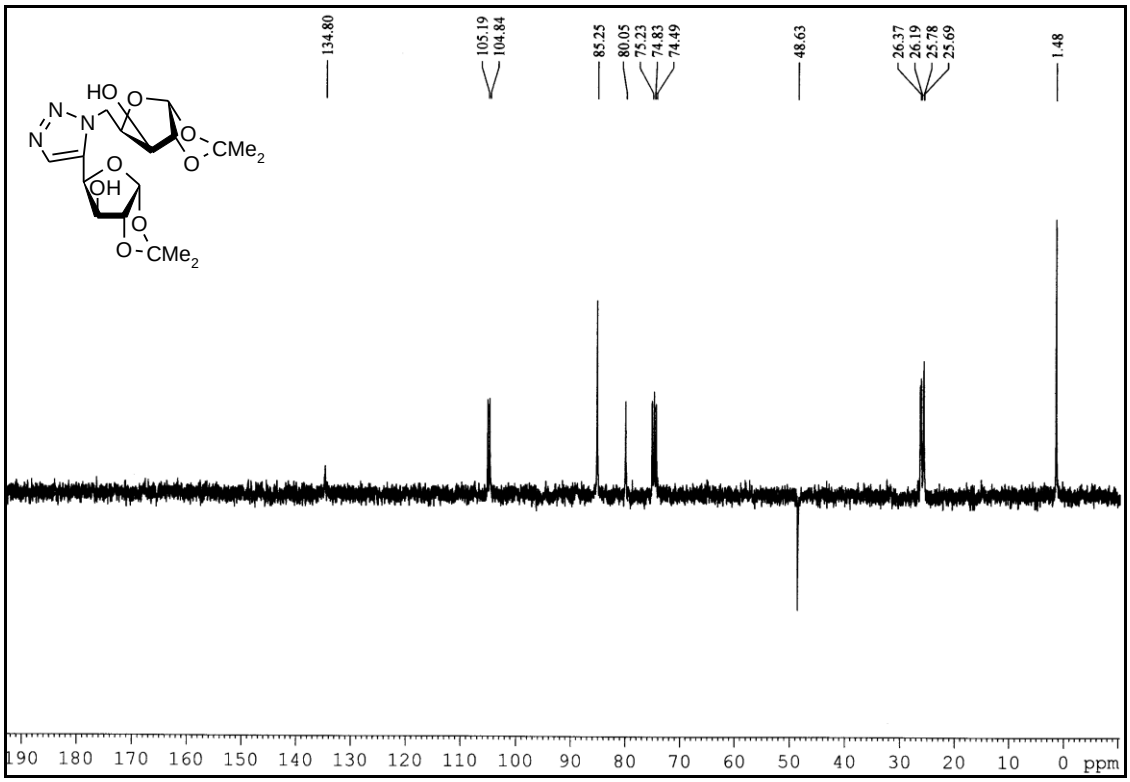

^{1}H NMR spectrum of 2

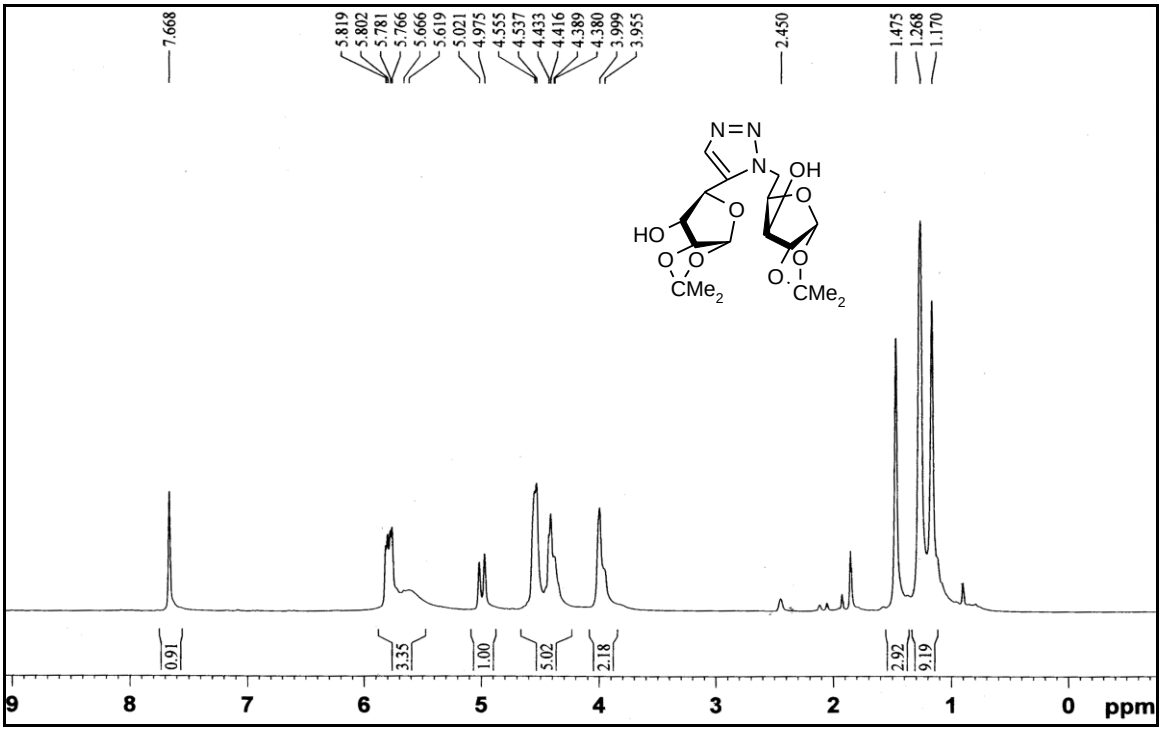

^{13}C NMR spectrum of 2

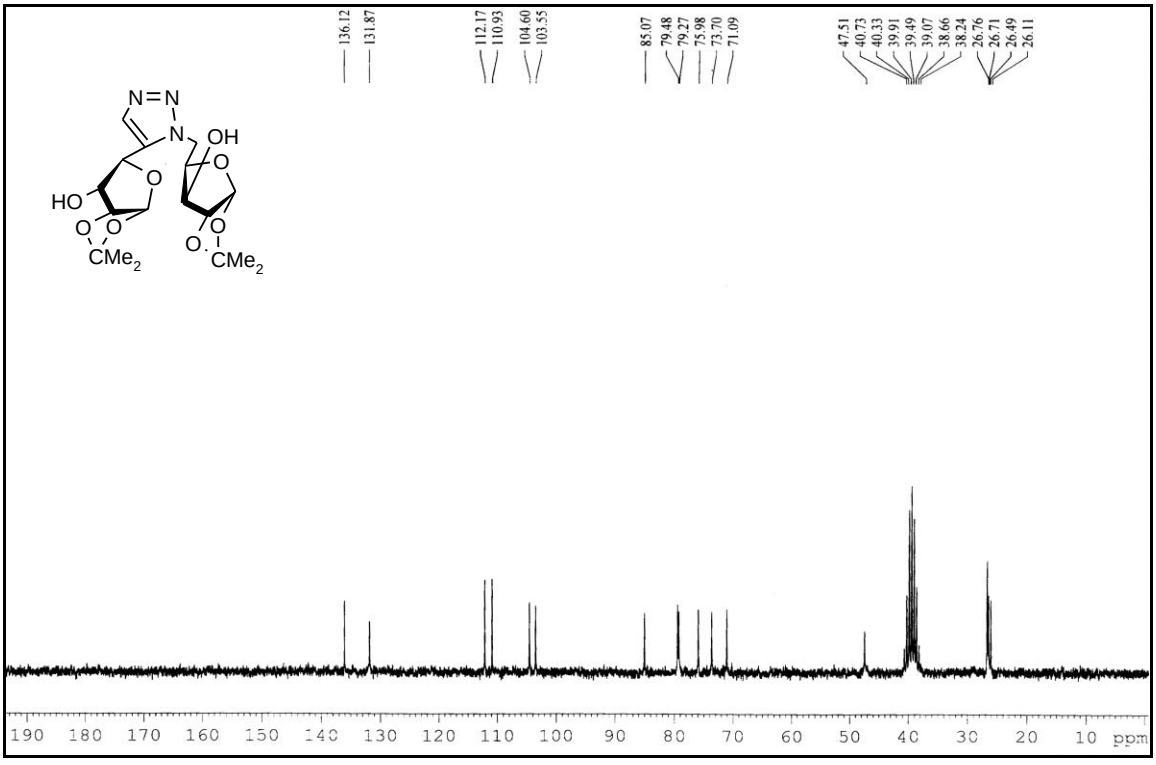

DEPT spectrum of 2

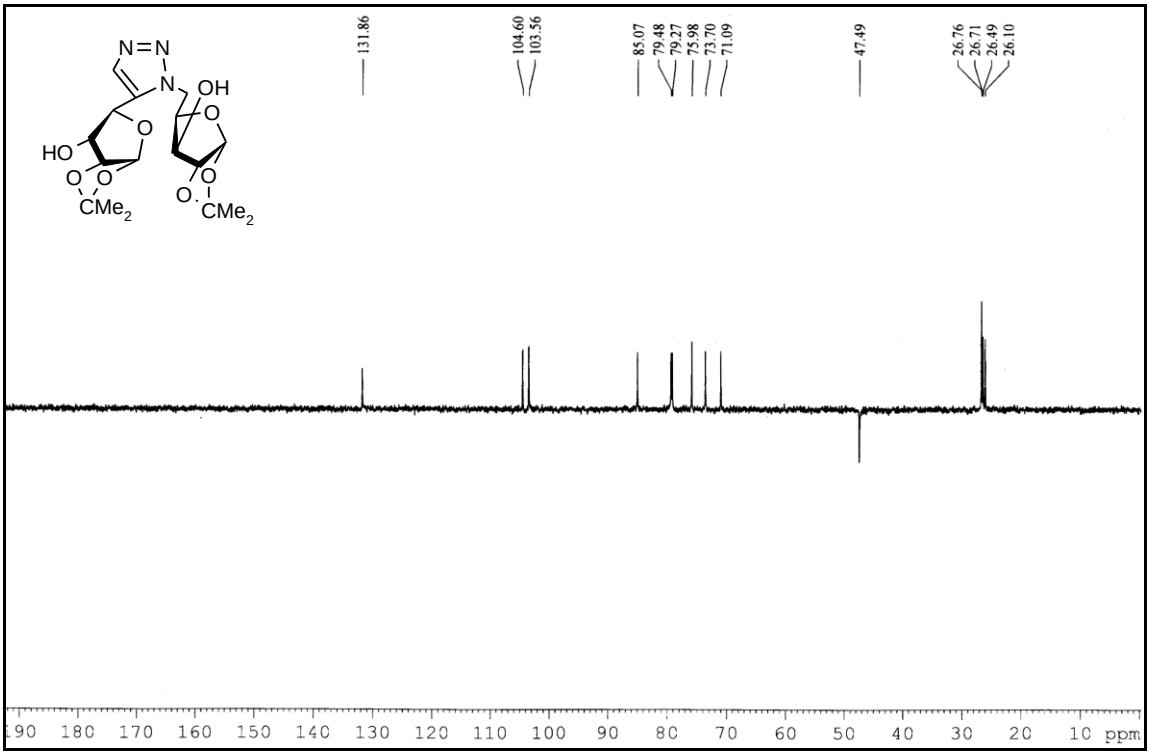

^{1}H NMR spectrum of 3

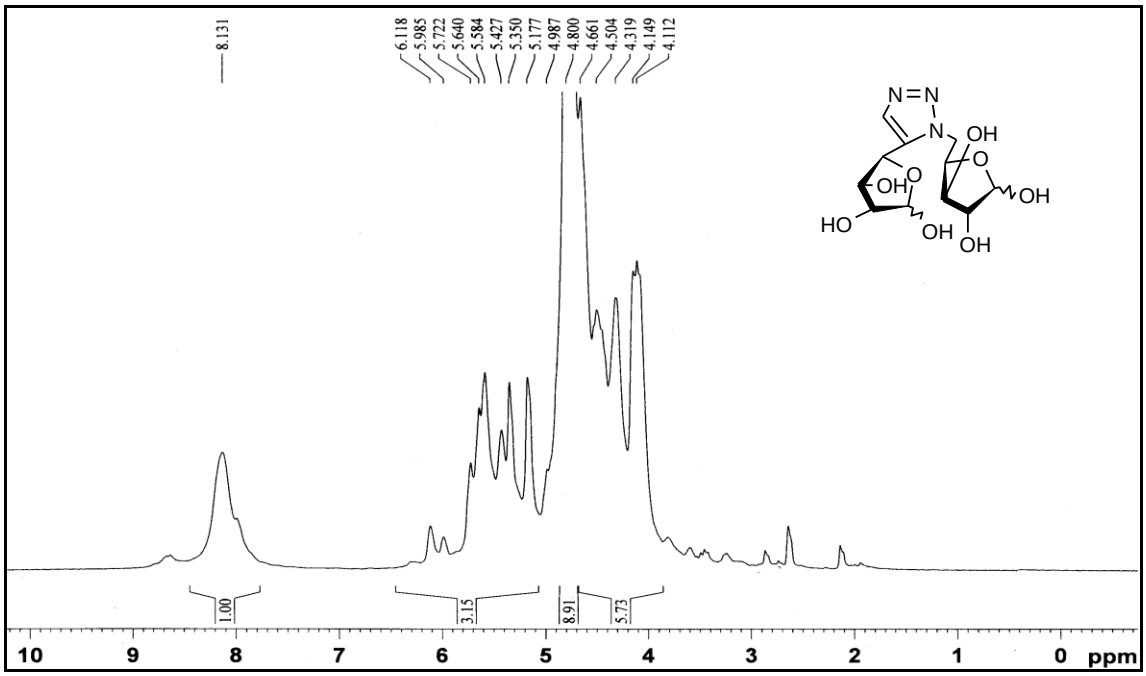

^{13}C NMR spectrum of 3

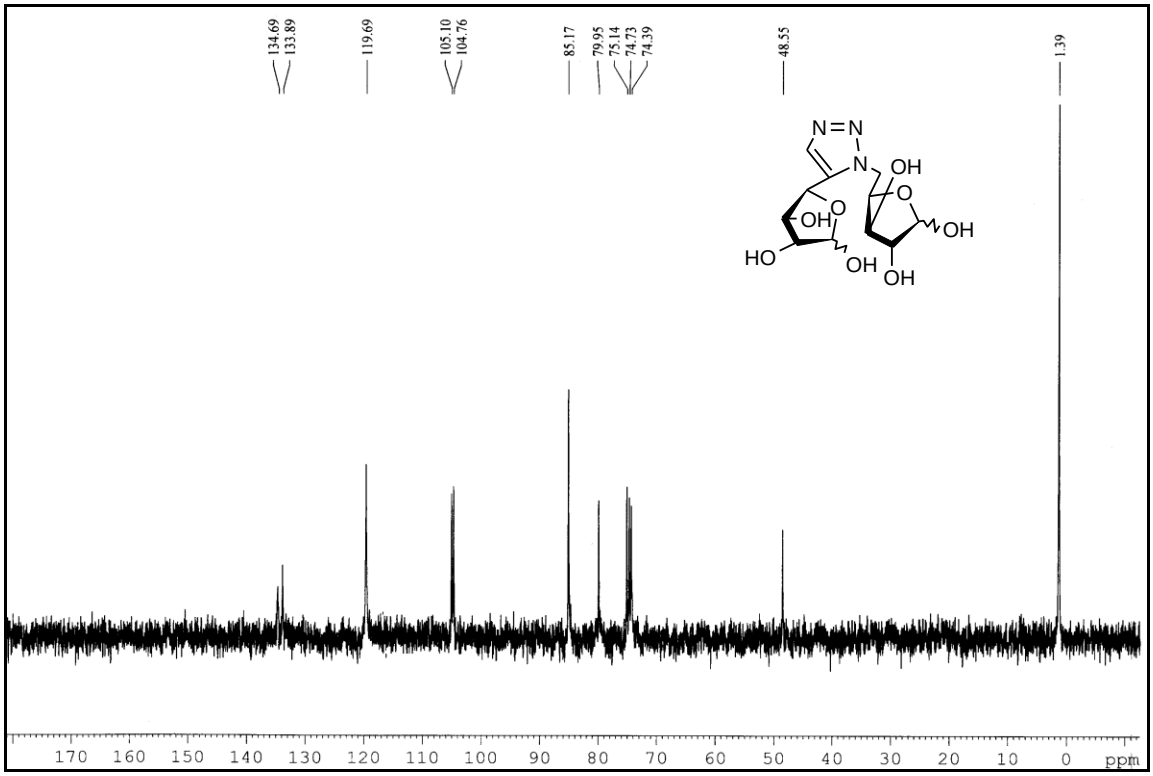

DEPT spectrum of 3

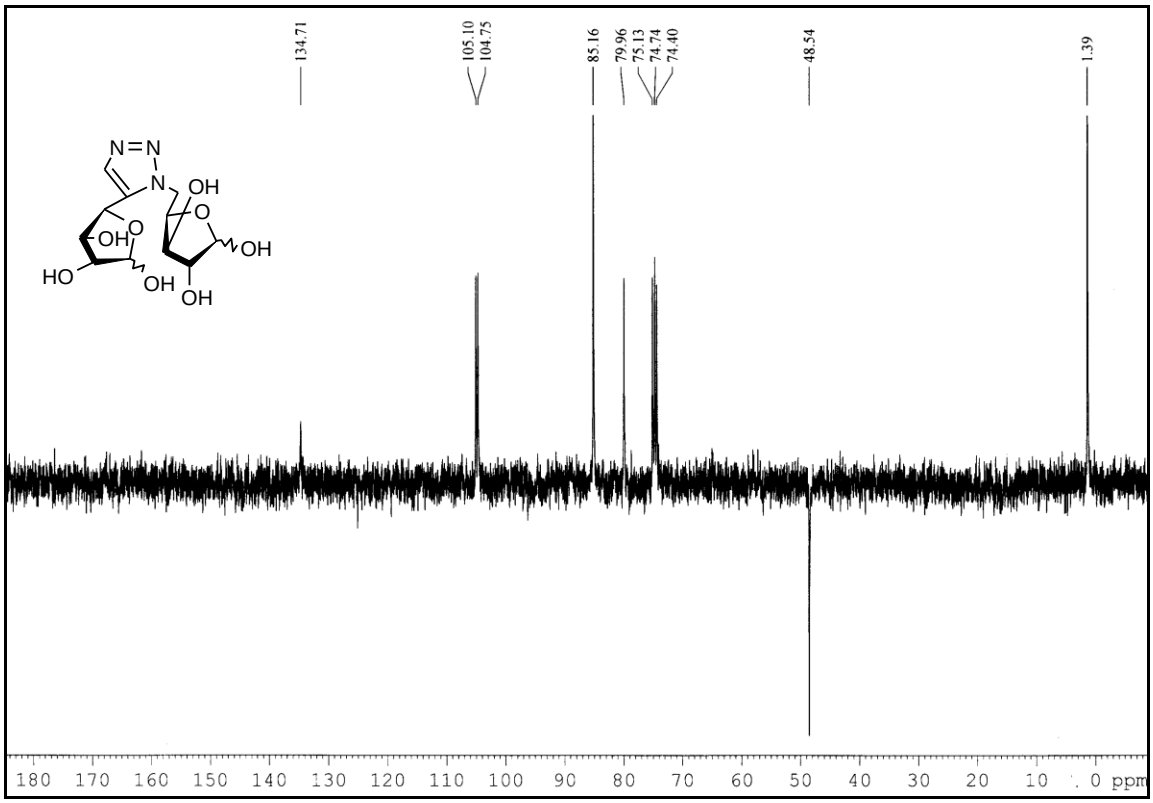

^{1}H NMR spectrum of 4

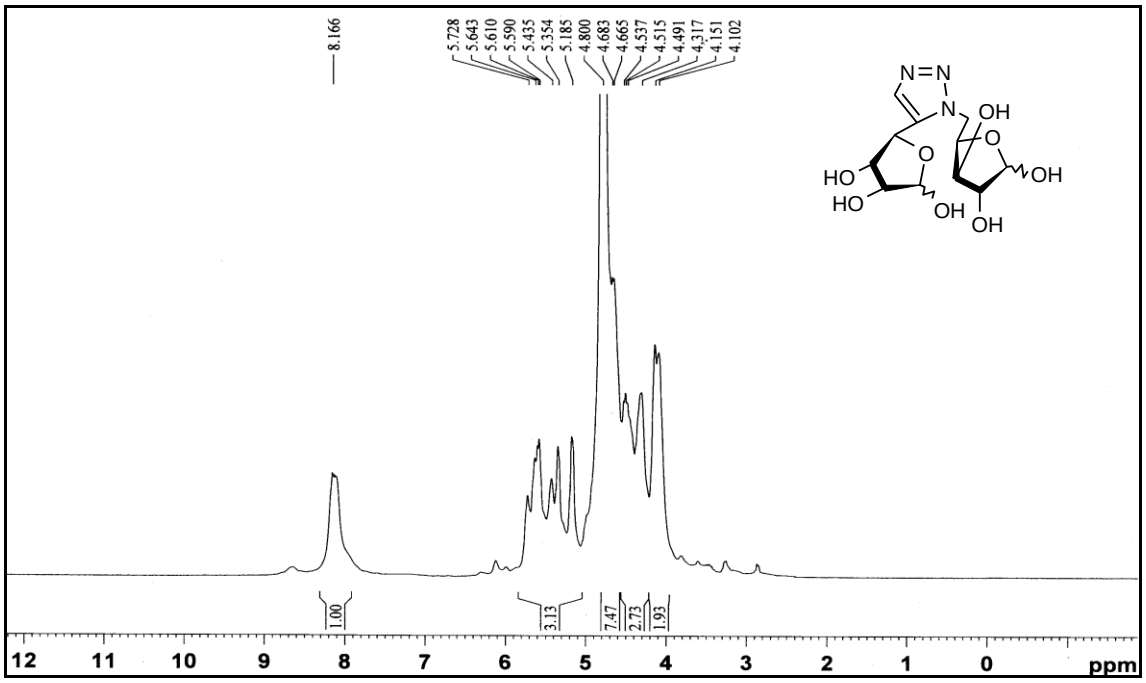

^{13}C NMR spectrum of 4

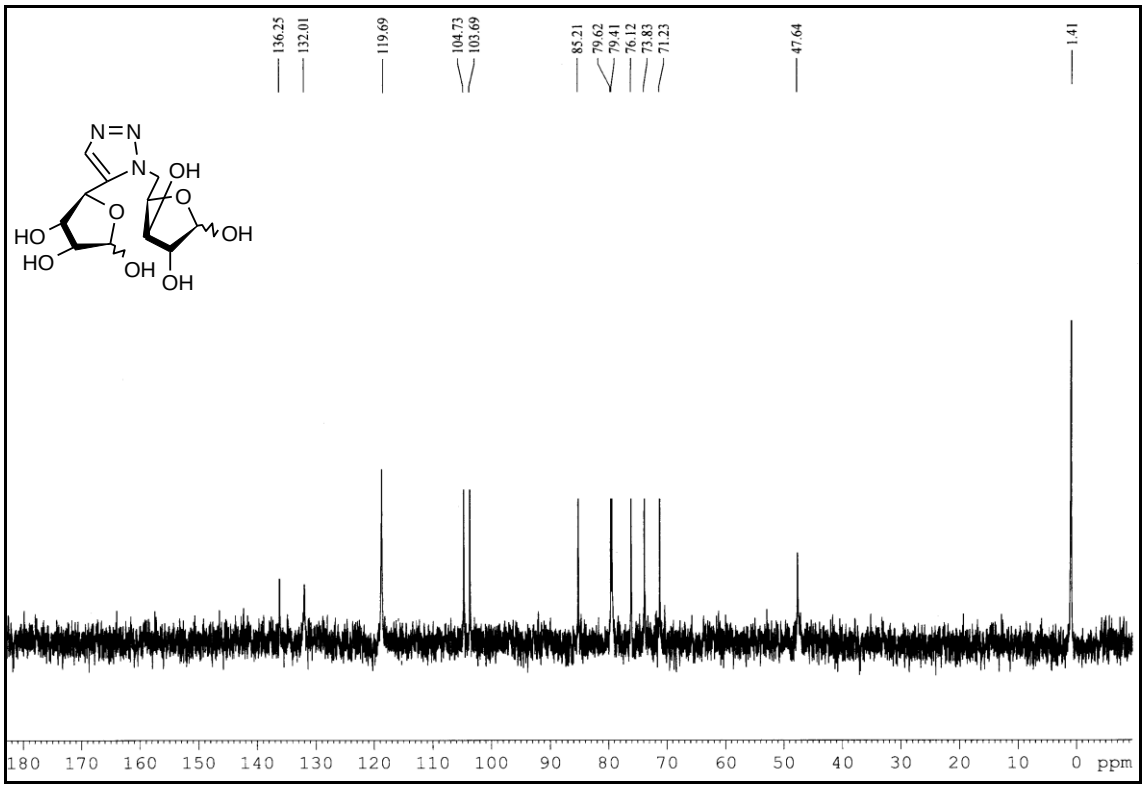

DEPT spectrum of 4

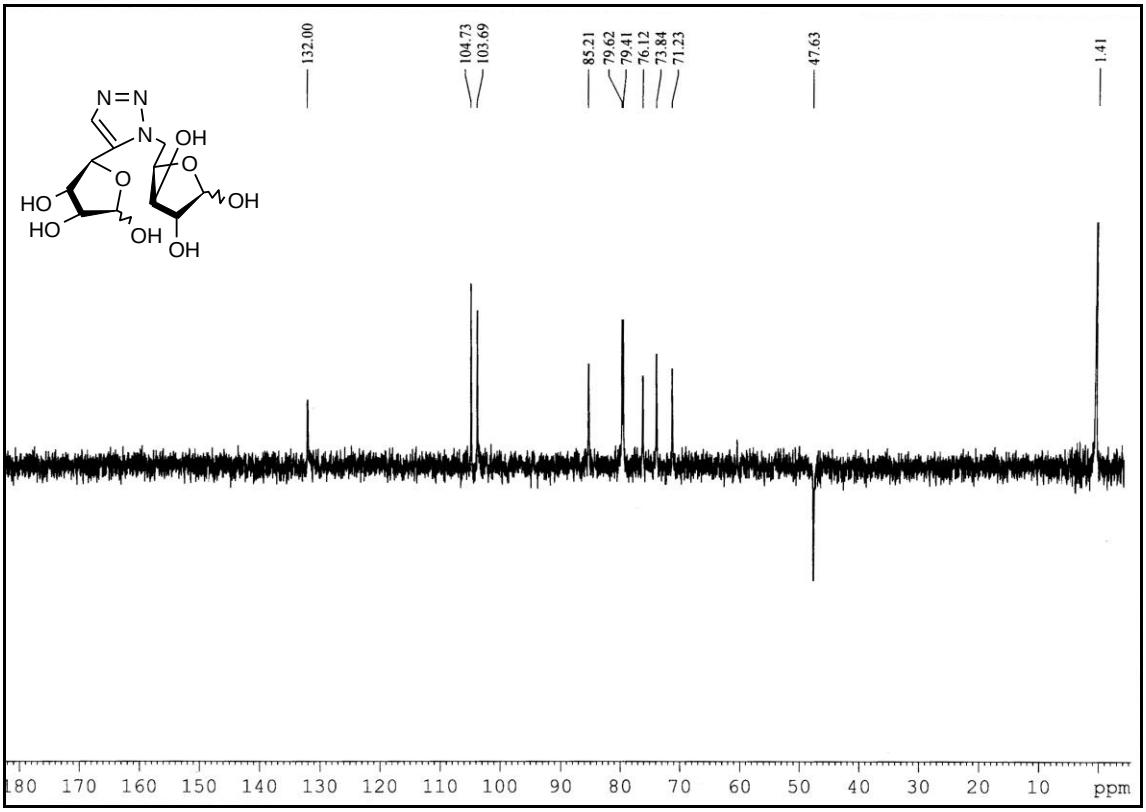

Synthesis of silver nanoparticles (AgNPs): An aqueous solution of compound **3** was mixed with aqueous solution of silver nitrate ($AgNO_3$) and stirred vigorously at room temperature for 5 minutes. After 5 minutes aqueous diethyl amine (Et_2NH) was added and again stirred vigorously at room temperature for another 10 minutes. So, after 15 minutes a yellow colored suspension was observed. Then the reaction condition was optimized by changing the concentration of compound **3**, $AgNO_3$ and Et_2NH respectively. From the optimized reaction condition it was observed that for a particular concentration of compound **3** (3 mM or 5 mM), the optimum concentration of $AgNO_3$ was 10 mM and Et_2NH was 50 mM. This optimized reaction condition was employed for the synthesis of AgNPs from compound **4**. In case of compound **4**, the reaction time was 25 minutes and a brown colored suspension was obtained. The yellow and brown colored suspensions (Figure 2-ESI) primarily indicated the formation of AgNPs. The details of the reaction parameters are shown in Table 1-ESI.

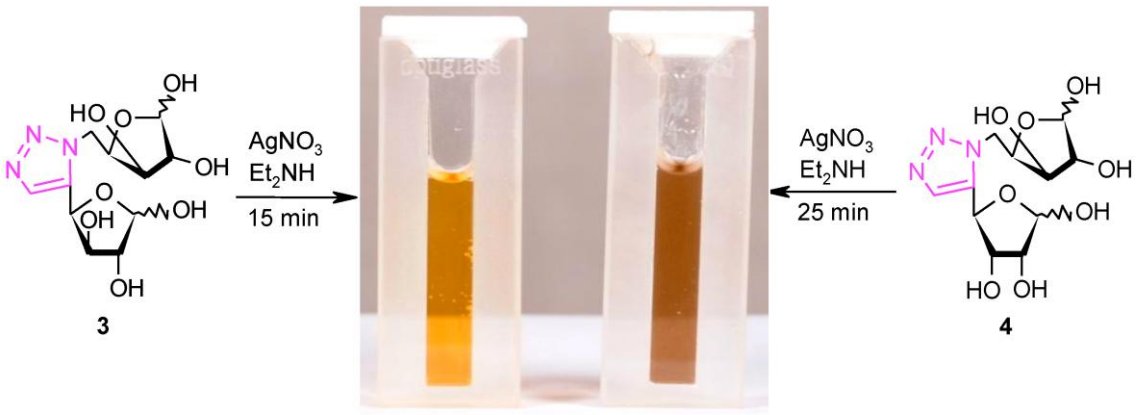

Figure 2-ESI: Photograph of AgNPs formed from **3** and **4**

Table 1-ESI: Details of the reaction parameters used in the silver nanoparticle synthesis and λ_{max} observed for nano silver suspension.

Triazole	Conc of Triazole (mM)	Conc of $AgNO_3$ (mM)	Conc of Et_2NH (mM)	Reaction time (min)	λ_{max} (nm)	AgNPs (Suspension)
3	5	10	75	15	405	a
3	5	10	50	15	406	a
3	5	10	25	60	-	b
3	5	5	50	60	-	b
3	5	10	50	15	406	a
3	5	20	50	60	-	b
3	3	10	50	15	403	a
3	5	10	50	15	405	a
4	3	10	50	25	410	a
4	5	10	50	25	408	a
a = suspension; b = not formed						

Characterization of AgNPs:

The yellow and brown colored suspensions indicated the formation of AgNPs. The AgNPs were characterized by UV-visible (UV-vis) spectroscopy measurements (Figure 3-ESI), Transmission electron microscopy (TEM) measurements (Figure 4-ESI and 5-ESI) and Scanning electron microscopy (SEM) measurements (Figure 6-ESI).

UV-vis spectroscopic studies: The optical properties of silver nanoparticle suspensions (samples **3** and **4**) were monitored on a Perkin-Elmer UV-vis Lambda 2 spectrophotometer.

Transmission electron microscopy (TEM) measurements: TEM measurements were performed on a FEI-TECNAI G220S-TWIN (Type-5022/22) instrument operating at an accelerating voltage of 200 kV. Samples for TEM studies were prepared by placing drops of the silver nanoparticle solutions of samples **3** and **4** on carbon-coated TEM grids. The films on the TEM grids were allowed to dry in air for 2 min following which the extra solution was removed using a blotting paper.

Scanning electron microscopy (SEM) measurements: SEM measurements were performed on a JEOL model 6400 instrument operating at an accelerating voltage of 20 kV. SEM samples were prepared by dispersing silver nanoparticle suspensions of samples **3** and **4** onto carbon coated aluminum SEM mounts. The films on the carbon coated aluminum SEM mounts were allowed to dry in air for 2 min following which the extra solution was removed.

UV-vis spectra: From the UV-vis spectra (Figure 3A-ESI and 3B-ESI) it was observed that the yellow colored suspension showed absorption band with a maximum of 403-406 nm and brown colored suspension showed absorption band with a maximum of 408-410 nm indicating the formation of AgNPs.

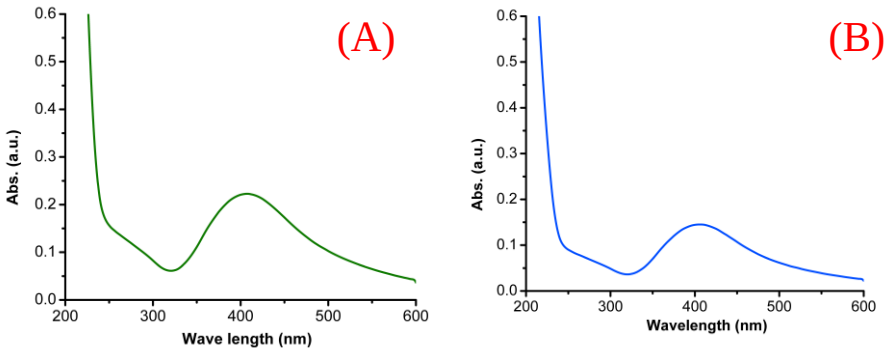

Figure 3A-ESI: UV-visible spectra of the AgNPs synthesized from (A) **3** of 5 mM and (B) **4** of 5 mM concentrations respectively (high diluted AgNP solutions).

Although a high diluted solution containing AgNPs elicited characteristic UV-vis spectra (Figure 3A-ESI; λ_{max} = 405nm), corresponding spectra were recorded at higher concentrations for better shape and peak positioning (Figure 5B-ESI).

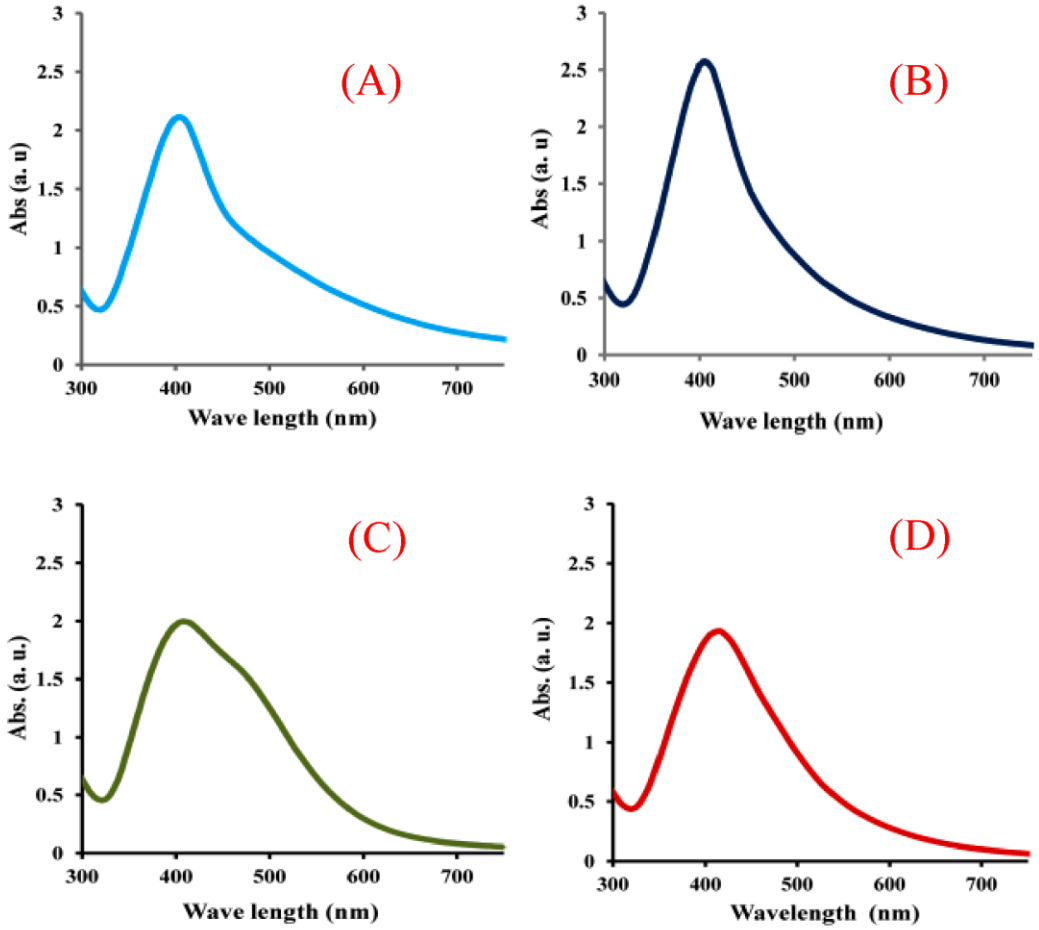

Figure 3B-ESI: UV-visible spectra of the AgNPs synthesized from (A) **3** of 3 mM, (B) **3** of 5 mM, (C) **4** of 3 mM and (D) **4** of 5 mM concentrations respectively (concentrated AgNP solutions).

TEM measurement: After characterization the AgNPs by means of UV-vis spectra (Figure 3-ESI), the size and morphology of the nanoparticles were characterized by TEM measurements (Figure 4-ESI and 5-ESI). From the TEM measurements it was observed that when the

concentration of compound **3** was 3 mM, then the shape of most of the AgNPs were octagonal (Figure 4-ESI). With increasing concentration of the compound **3** from 3 mM to 5 mM the shape of the AgNPs changed from octagonal to spherical (Figure 4-ESI). But it was observed that, in case of compound **4**

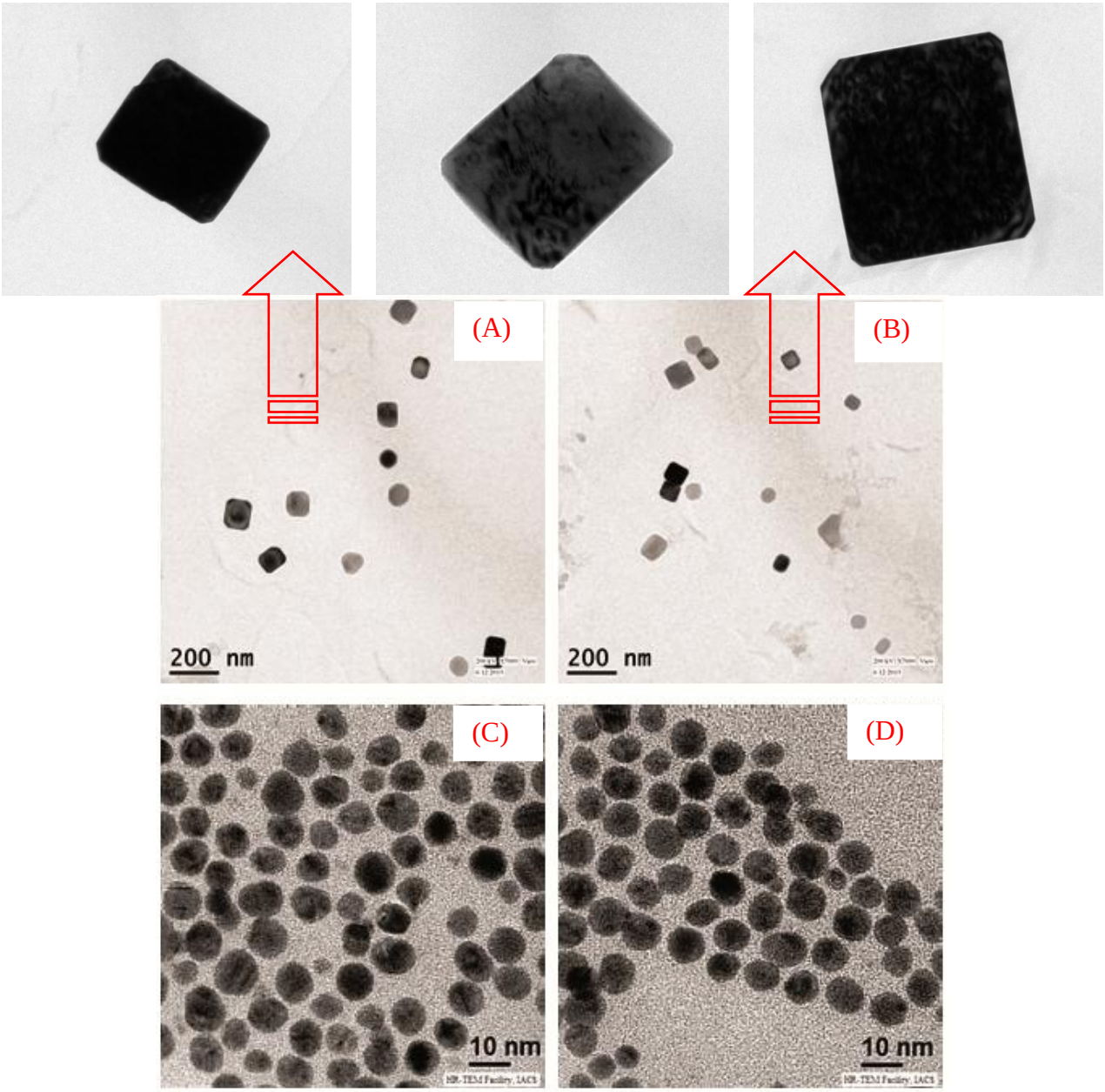

Figure 4-ESI: TEM images of AgNPs synthesized from (A & B) **3** of 3 mM (magnified in the panel above) and (C & D) **3** of 5 mM concentrations respectively.

both in 3 mM and 5 mM concentrations the shape of the AgNPs was not properly spherical (Figure 5-ESI).

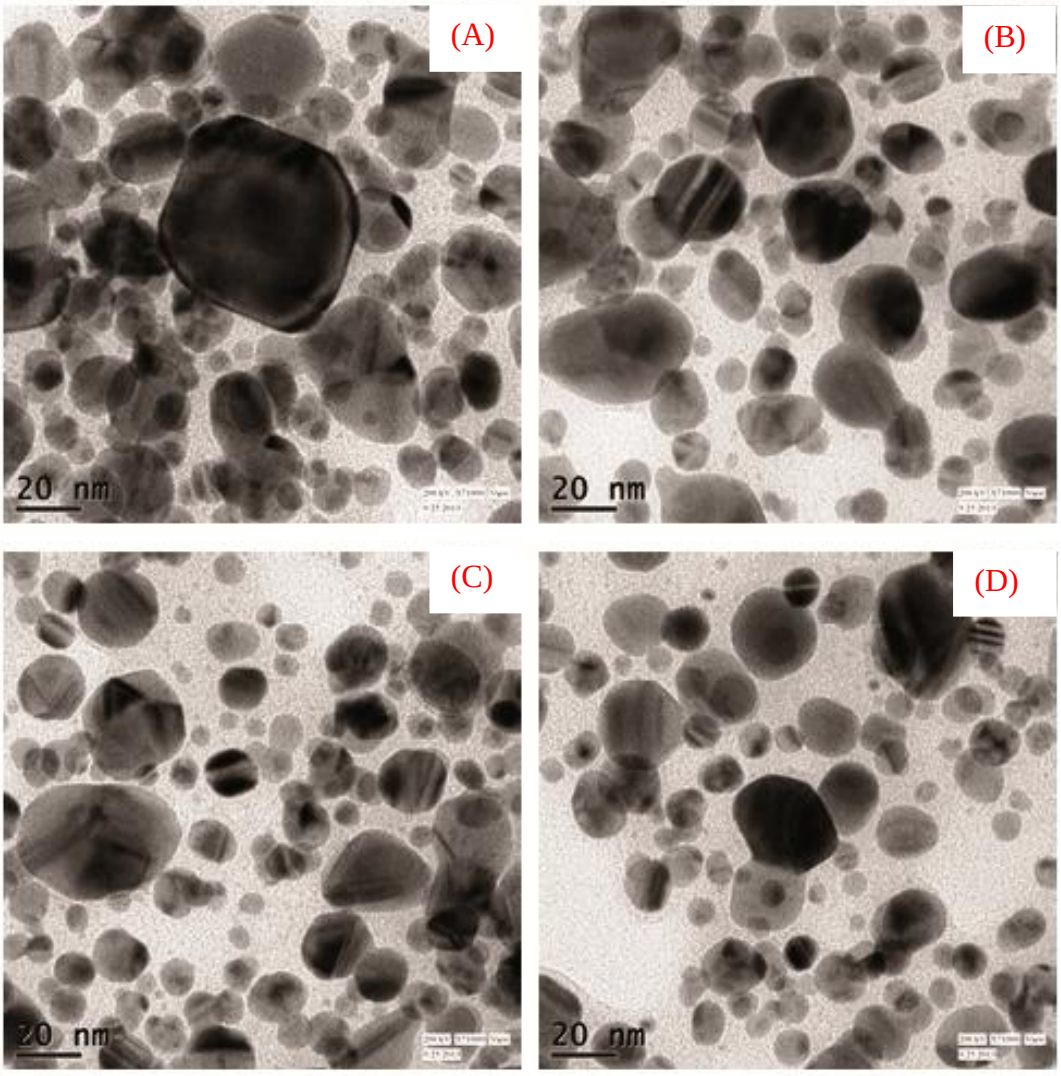

Figure 5-ESI: TEM images of AgNPs synthesized from (A & B) **4** of 3 mM and (C & D) **4** of 5 mM concentrations respectively.

SEM measurement: After characterization the size and morphology of AgNPs by TEM measurements (Figure 4-ESI and 5-ESI), the state of AgNPs were characterized by SEM measurements. From the SEM images it was observed that the AgNPs agglomerated with some dispersed nanoparticles (Figure 6-ESI).

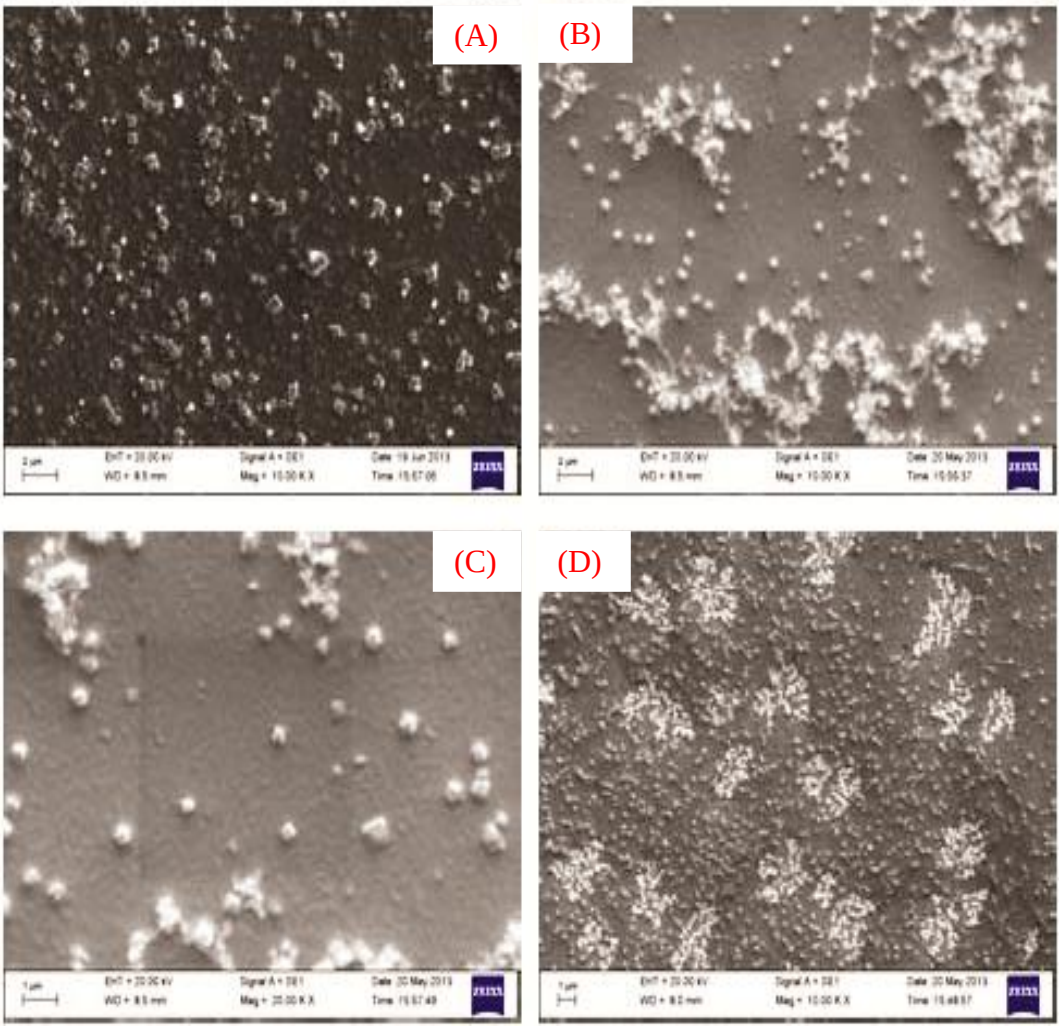

Figure 6-ESI: ZEISS-SEM images of the AgNPs synthesized from (A) **3** of 3 mM, (B) **3** of 5 mM, (C) **4** of 3 mM and (D) **4** of 5 mM concentrations respectively.

Study of templeting effect of triazole ring: 1,2,3-Triazoles are known for their metal binding properties.[4] The binding of Ag^{+} with the triazole ring was established in case of **1** and **2** by

conducting ^{1}H and ^{13}C NMR study. From the proton NMR study, it was observed that the triazole proton of **1** (Scheme 1-ESI) shifted towards downfield with the addition of $AgNO_3$. When no $AgNO_3$ was added to compound **1**, the triazole proton resonated at 7.801 ppm. When 1:0.5, 1:1 and 1:2 of **1** and $AgNO_3$ were used for this study, then the triazole proton of **1** shifted from 7.801-7.806 ppm, 7.801-7.814 ppm and 7.801-7.816 ppm (Figure 7A-ESI). So, it was obvious that the 1:1 mixture of **1** and $AgNO_3$ resulted in a maximum downfield shifting (0.013 ppm; 5.2 Hz) of the triazole proton of **1**. As we observed maximum downfield shift of triazolyl proton of 1:1 mixture of **1** and $AgNO_3$, we performed the ^{1}H NMR study for **2** using only 1:1 of compound **2** and $AgNO_3$ mixture (Figure 7B-ESI). For compound **2** it was observed that 1:1 mixture of **2** and $AgNO_3$ resulted a greater downfield shift (0.029 ppm; 11.6 Hz) of the triazole proton compared to **1** (5.2 Hz).

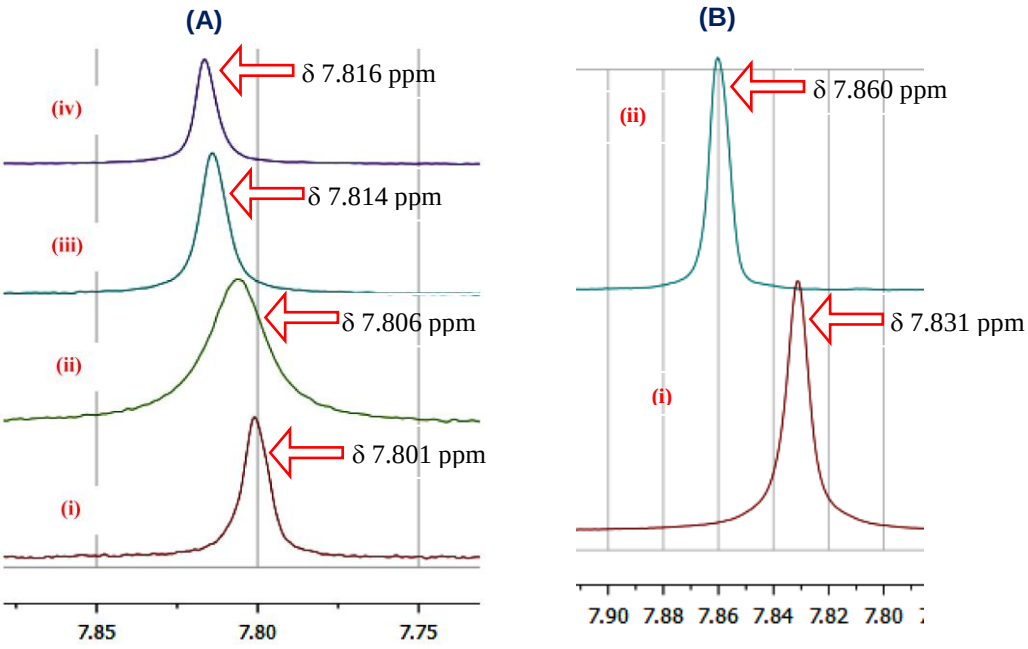

Figure 7-ESI: Comparison of ^{1}H NMR chemical shift of (A) triazole proton of **1** [image (i) for **1** only, (ii) for 1:0.5, (iii) for 1:1 and (iv) for 1:2 of **1** and $AgNO_3$ mixture respectively] and (B) triazole proton of **2** [image (i) for **2** only and (ii) for 1:1 of **2** and $AgNO_3$ mixture respectively].

The down field shifting of the triazolyl protons of both the compounds **1** and **2** encouraged us to conduct the ^{13}C NMR study. From the ^{13}C NMR studies it was observed that with the addition of $AgNO_3$ to the compound **1** (1:1 ratio), the C4 of the triazole ring shifted towards downfield (134.92 ppm to 135.31 ppm). So the downfield shifting of C4 of the triazole ring of **1** was 0.39 ppm; 58.5 Hz (Figure 8A-ESI). But in case of compound **2**, it was observed that in the 1:1 mixture of **2** and $AgNO_3$ the C4 of the triazole ring shifted towards downfield (133.49 ppm to 134.42 ppm). So the downfield shifting of C4 of the triazole ring of **2** was 0.93 ppm; 139.5 Hz (Figure 8B-ESI) which is higher compared to C4 of compound **1** (0.39 ppm; 58.5 Hz). So, from both ^{1}H and ^{13}C NMR studies it can be said that the interaction between Ag^{+} and the triazole ring was more efficient in case of compound **2** than **1**. The full ^{1}H and ^{13}C NMR spectra of the 1,5-DT linked disaccharides for templating effect with Ag^{+} for AgNPs formation are also shown below.

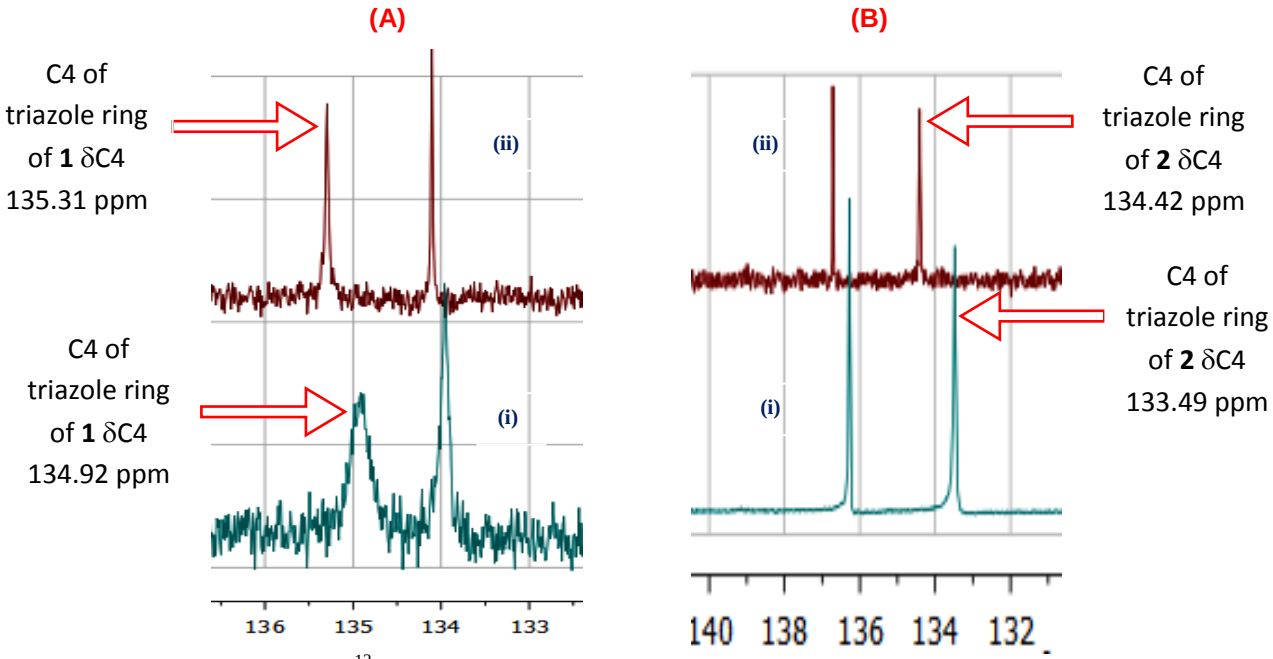

Figure 8-ESI: Comparison of ^{13}C NMR chemical shift of (A) C4 of triazole ring of **1** [image (i) for **1** only and image (ii) for 1:1 of **1** and $AgNO_3$ mixture] and (B) C4 of triazole ring of **2** [image (i) for **2** only and image (ii) for 1:1 of **2** and $AgNO_3$ mixture].

NMR spectra of templating effect of triazole ring:

^{1}H NMR spectrum of 1

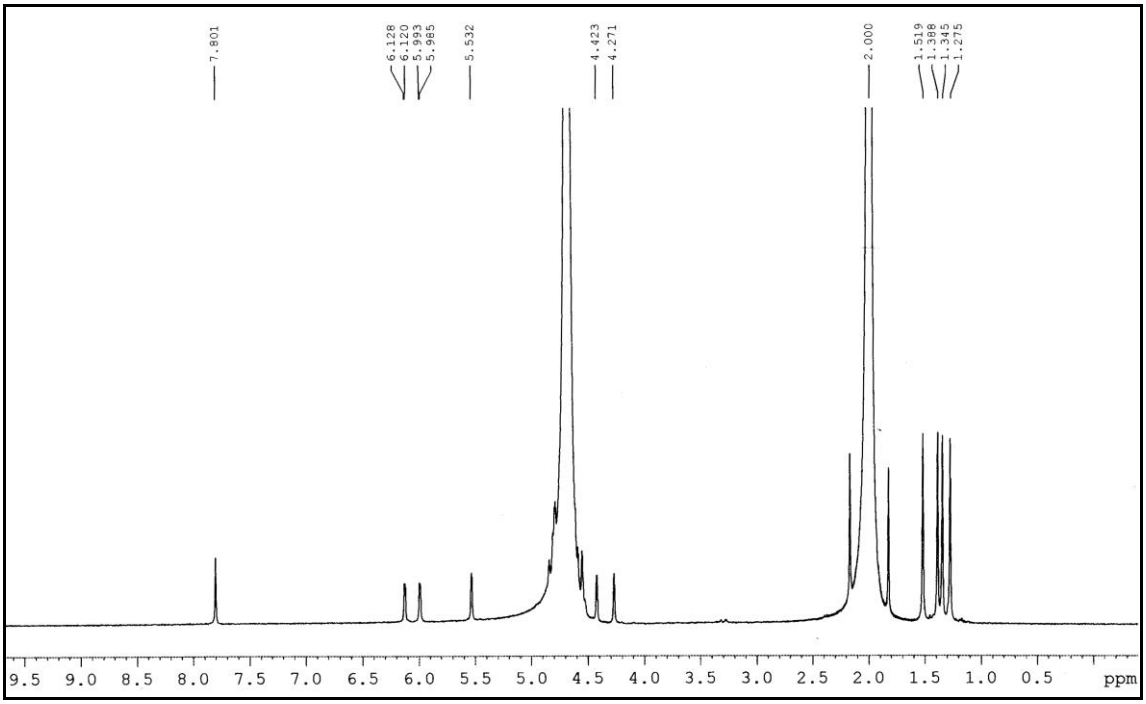

^{1}H NMR spectrum of 1:0.5 of 1 and $AgNO_3$ mixture

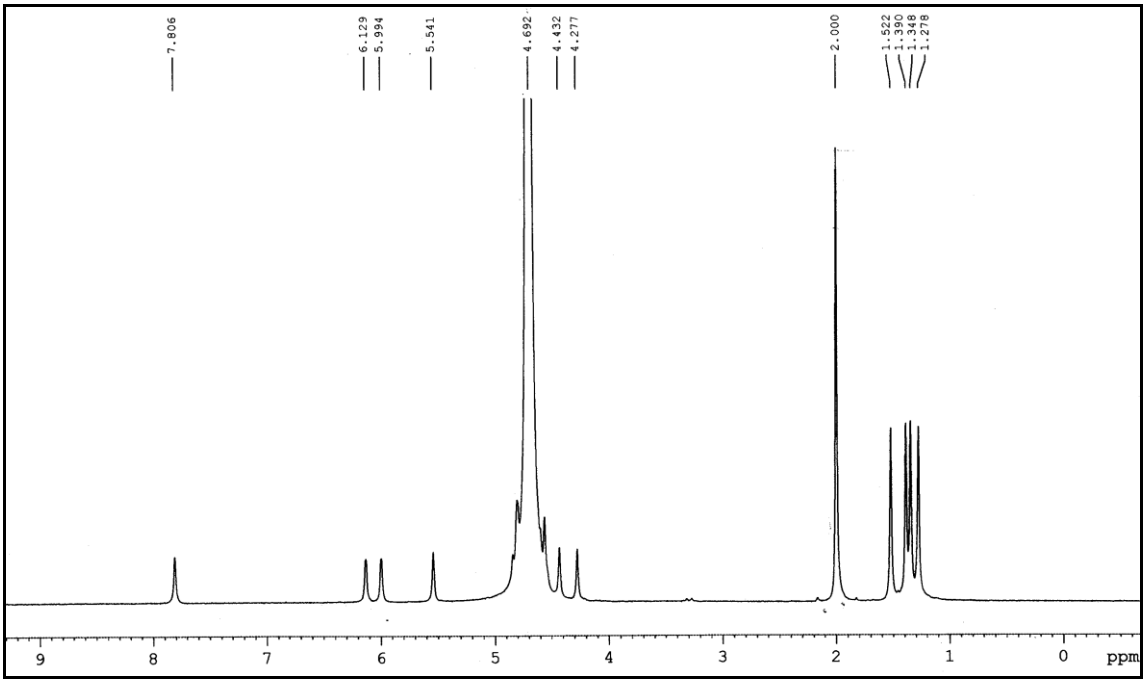

^{1}H NMR spectrum of 1:1 of **1 and $AgNO_3$ mixture**

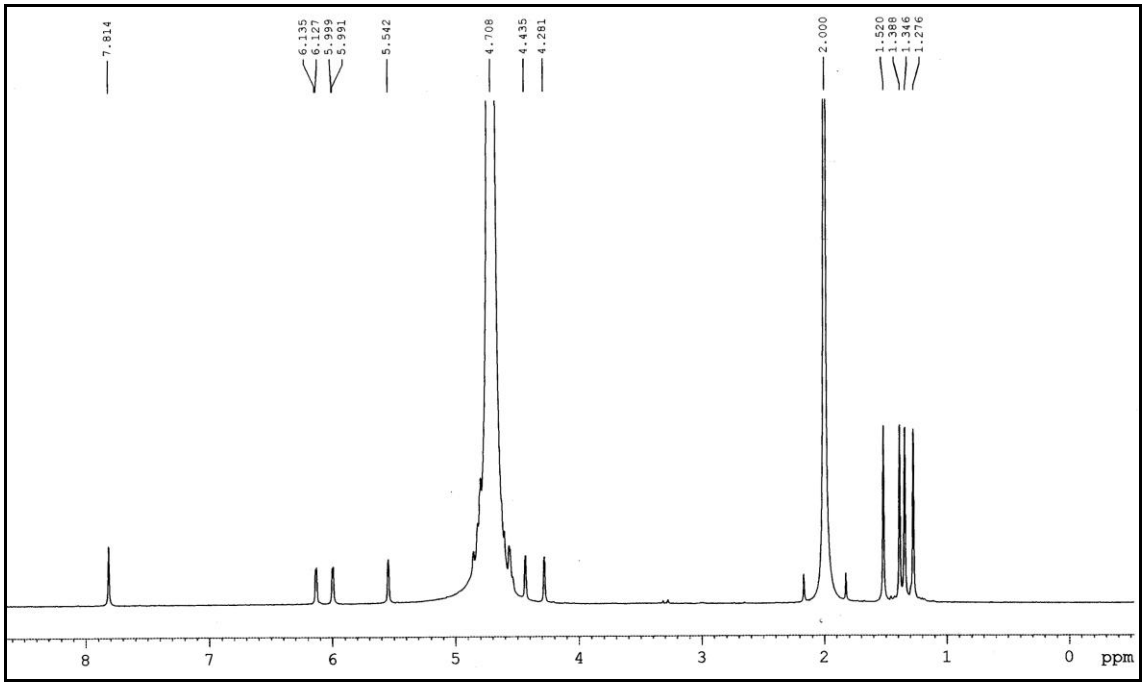

^{1}H NMR spectrum of 1:2 of 1 and $AgNO_3$ mixture

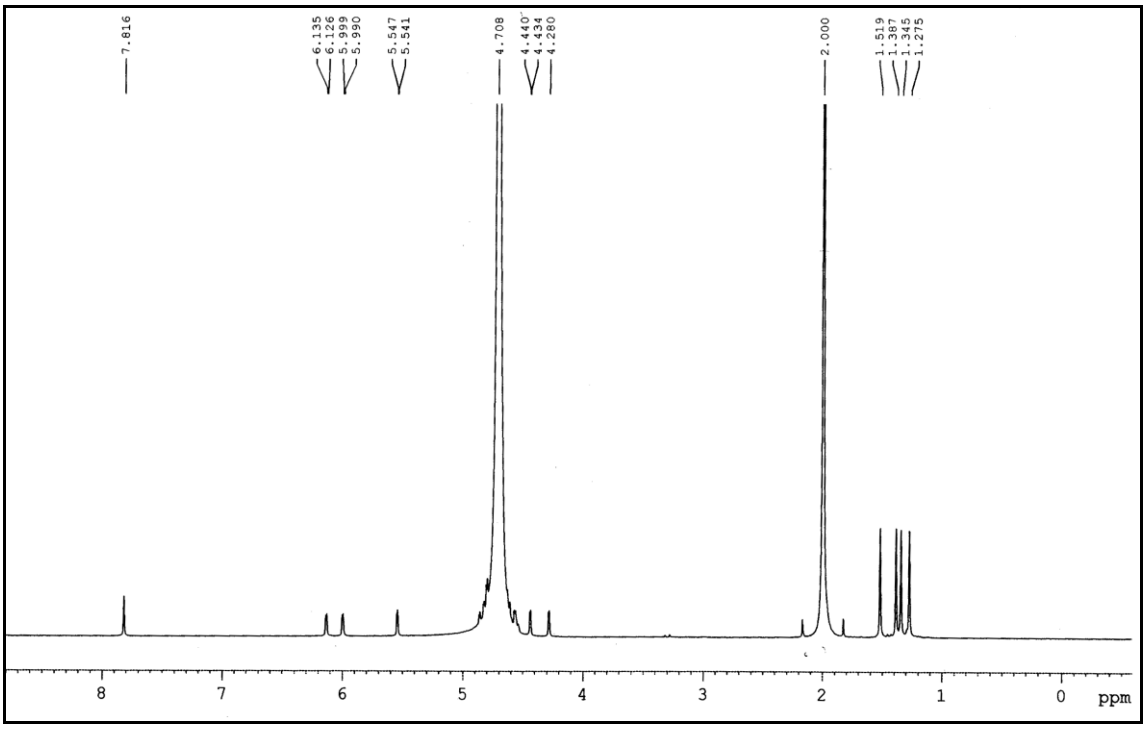

^{13}C NMR spectrum of 1

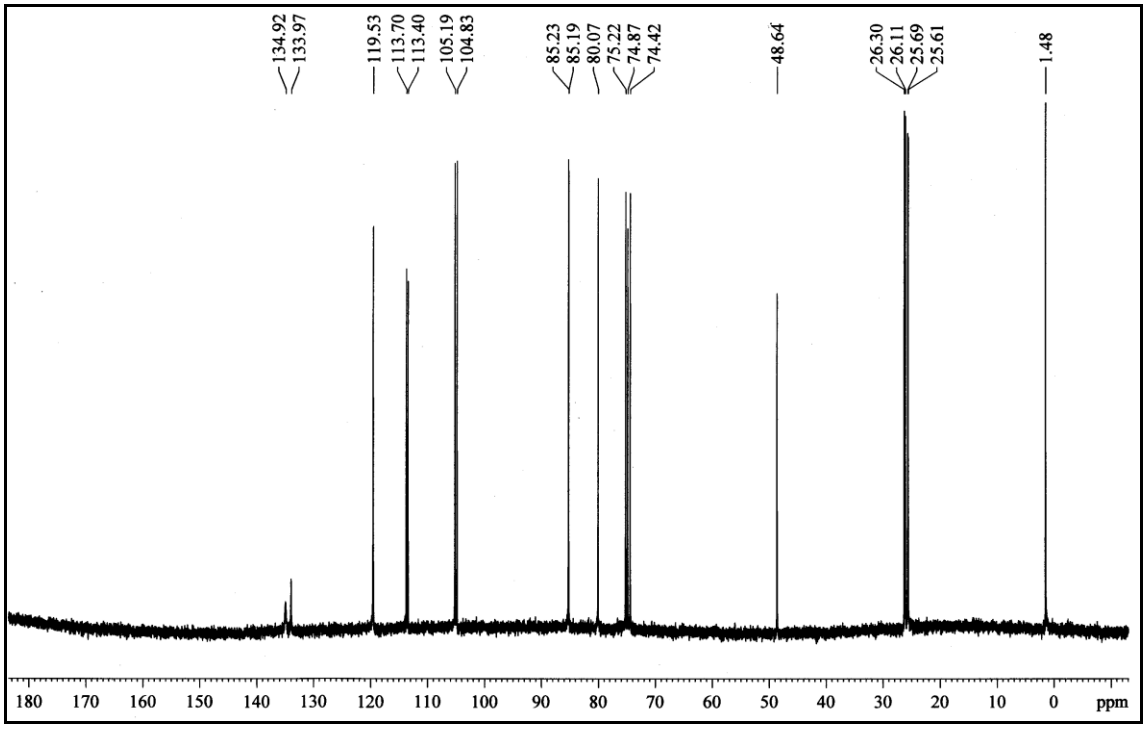

^{13}C NMR spectrum of 1:1 of 1 and $AgNO_3$ mixture

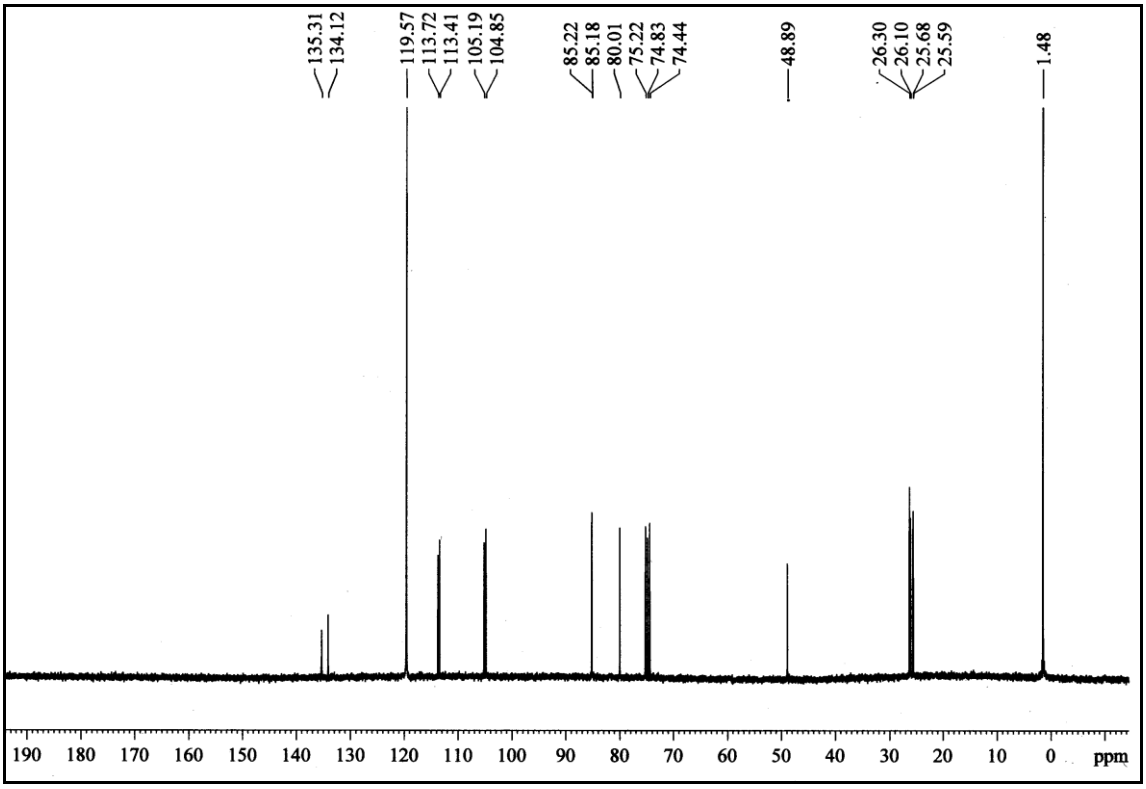

^{1}H NMR spectrum of 2

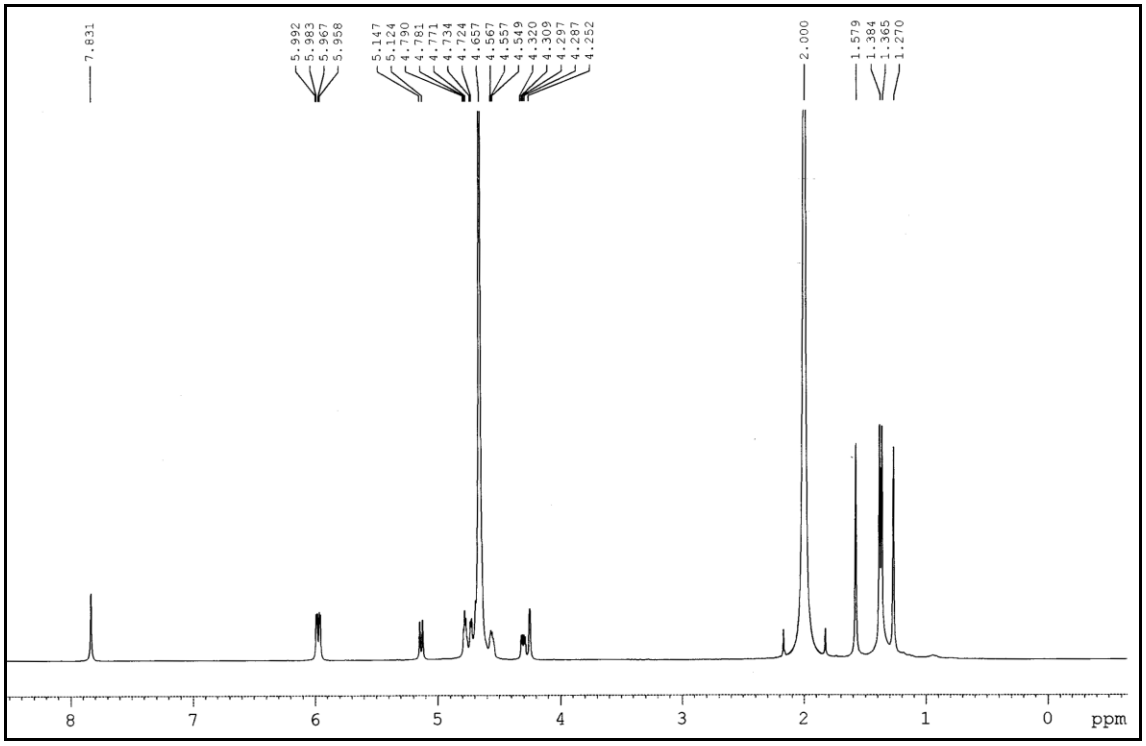

^{1}H NMR spectrum of 1:1 of 2 and $AgNO_3$ mixture

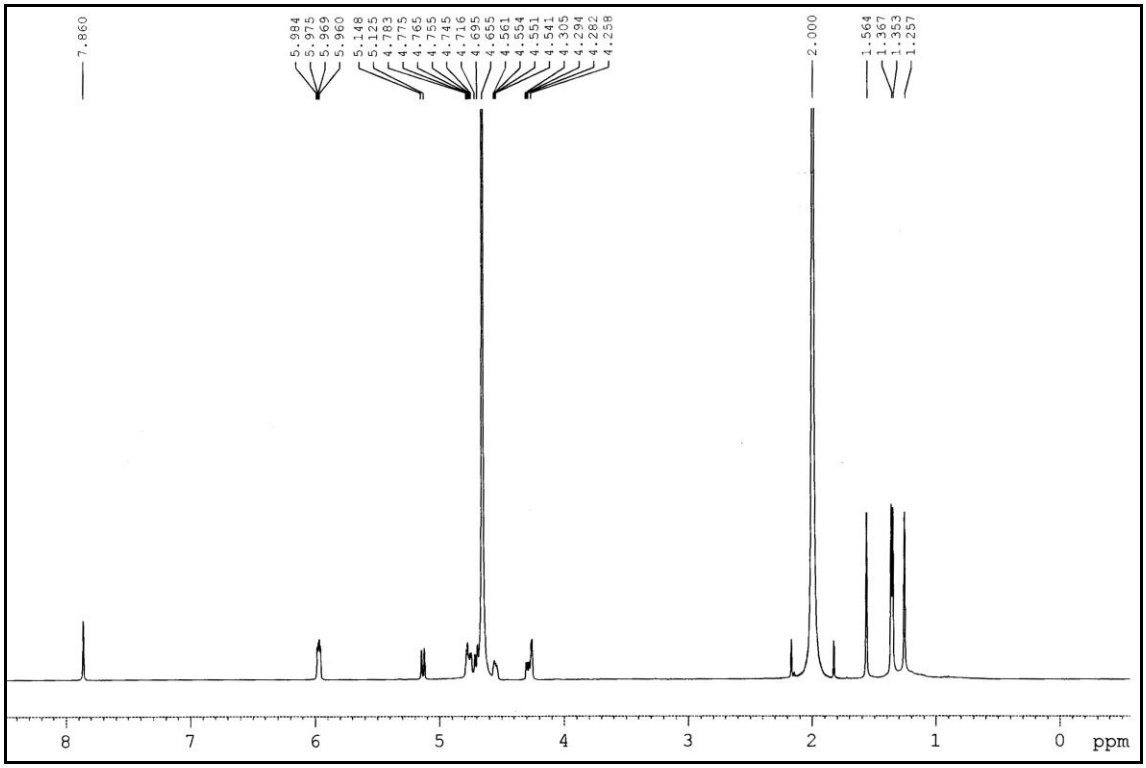

^{13}C NMR spectrum of 2

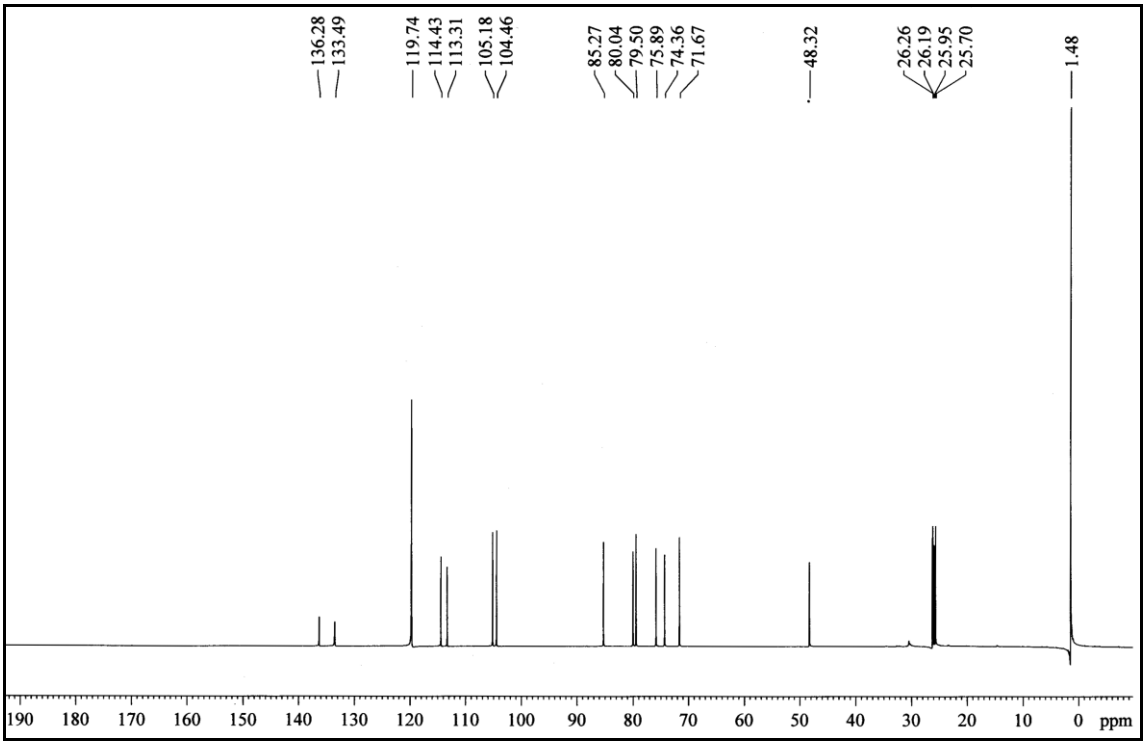

^{13}C NMR spectrum of 1:1 of 2 and $AgNO_3$ mixture

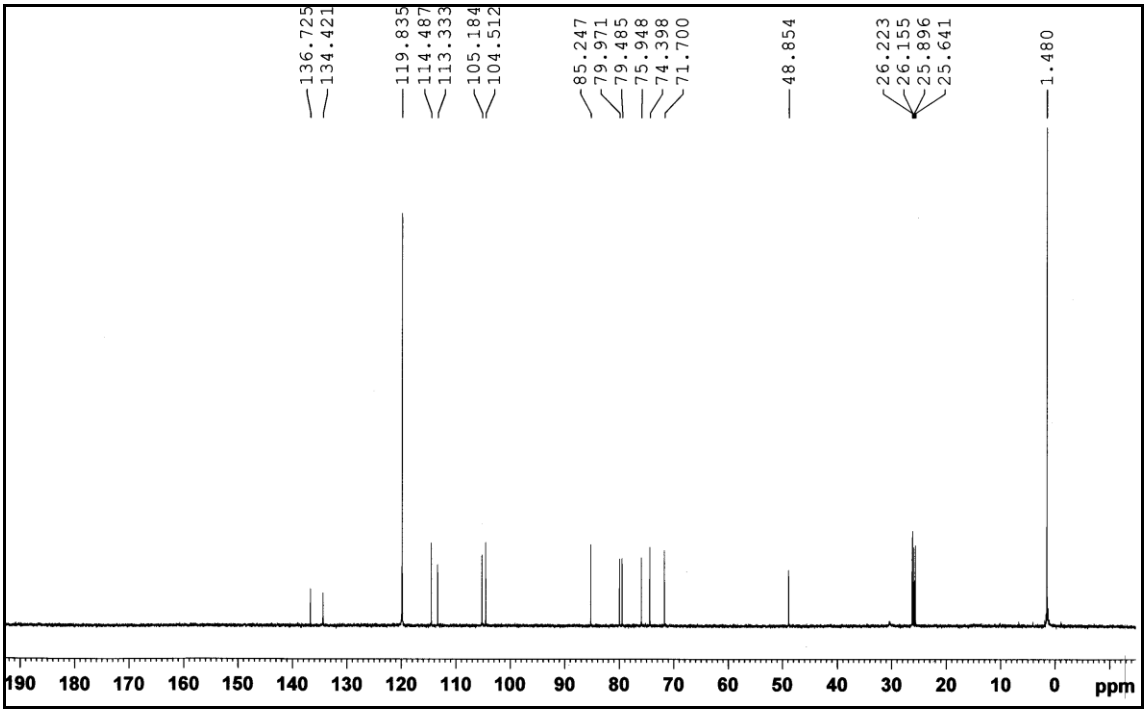

Formation of diacids 5 and 6: During the Ag^{+} to Ag^{0} conversion the reducing agents **3** and **4** would be oxidized into the corresponding acids **5** and **6**. The formation of the acids **5** and **6** were confirmed from HRMS analysis (Figure 9A-ESI and 9B-ESI). The peak at 352.0927 corresponds to the acid **5** (Figure 13A-ESI). On the other hand the peak at 352.1044 corresponds to the acid **6** (Figure 9B-ESI).

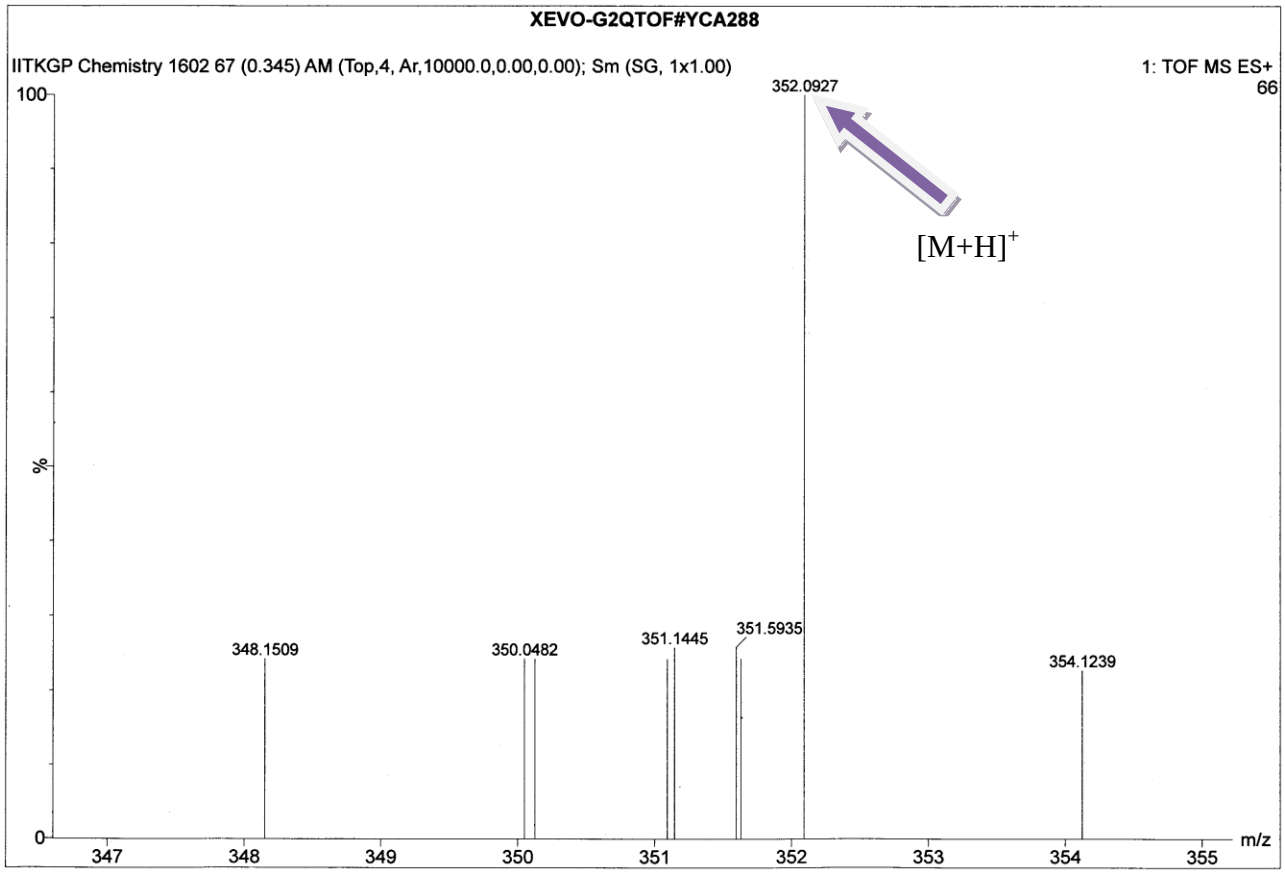

Figure 9A-ESI: HRMS (ESI^{+}) of di-acid **5** obtained from **3**.

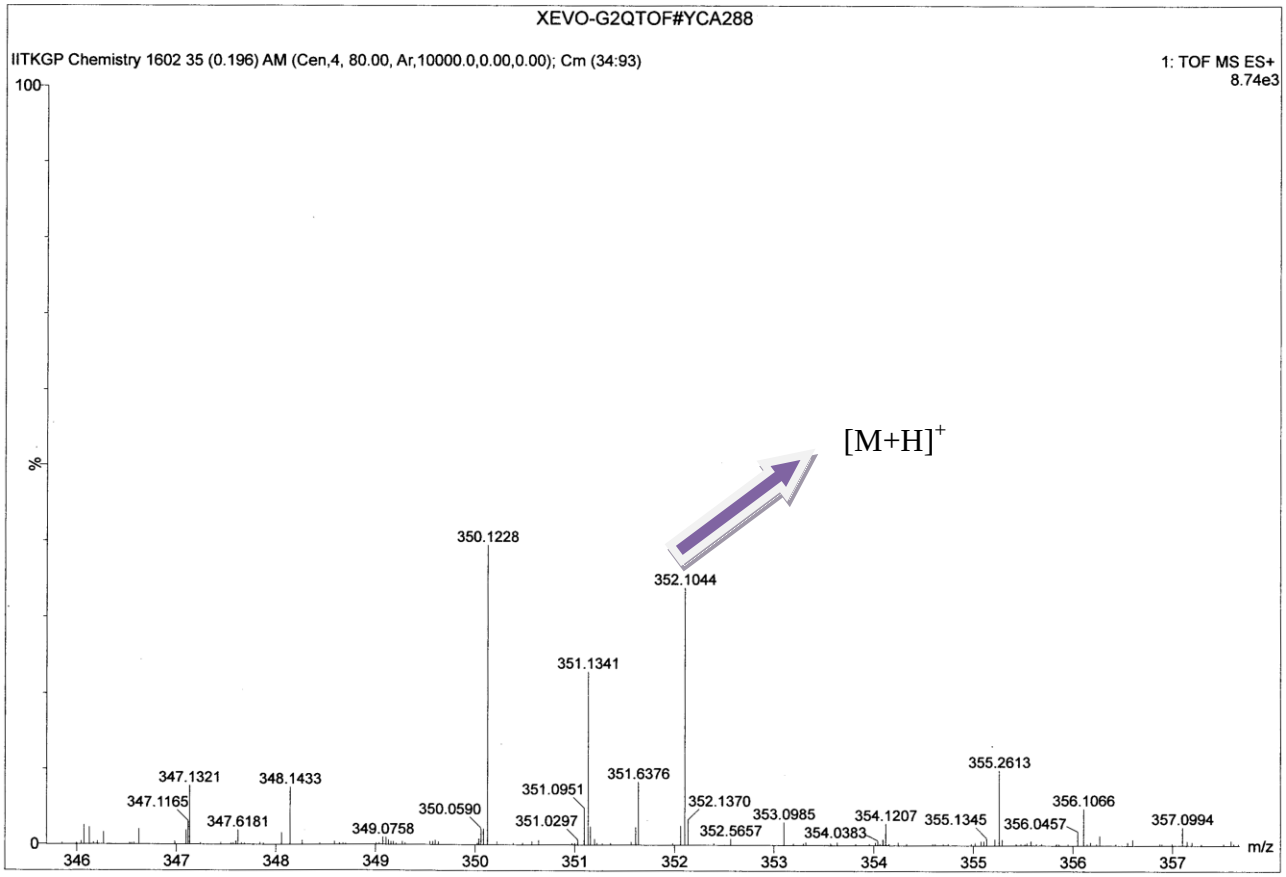

Figure 9B-ESI: HRMS (ESI^+) of di-acid **6** obtained from **4**.

Binding of silver with aldehydes 3 and 4: During the HRMS analysis for identifying the diacids **5** and **6**, peaks at 429.2293 and 428.0089 were observed which correspond to silver bound to aldehydes **3** and **4** (Figure **10A-ESI** and **10B-ESI**) respectively.

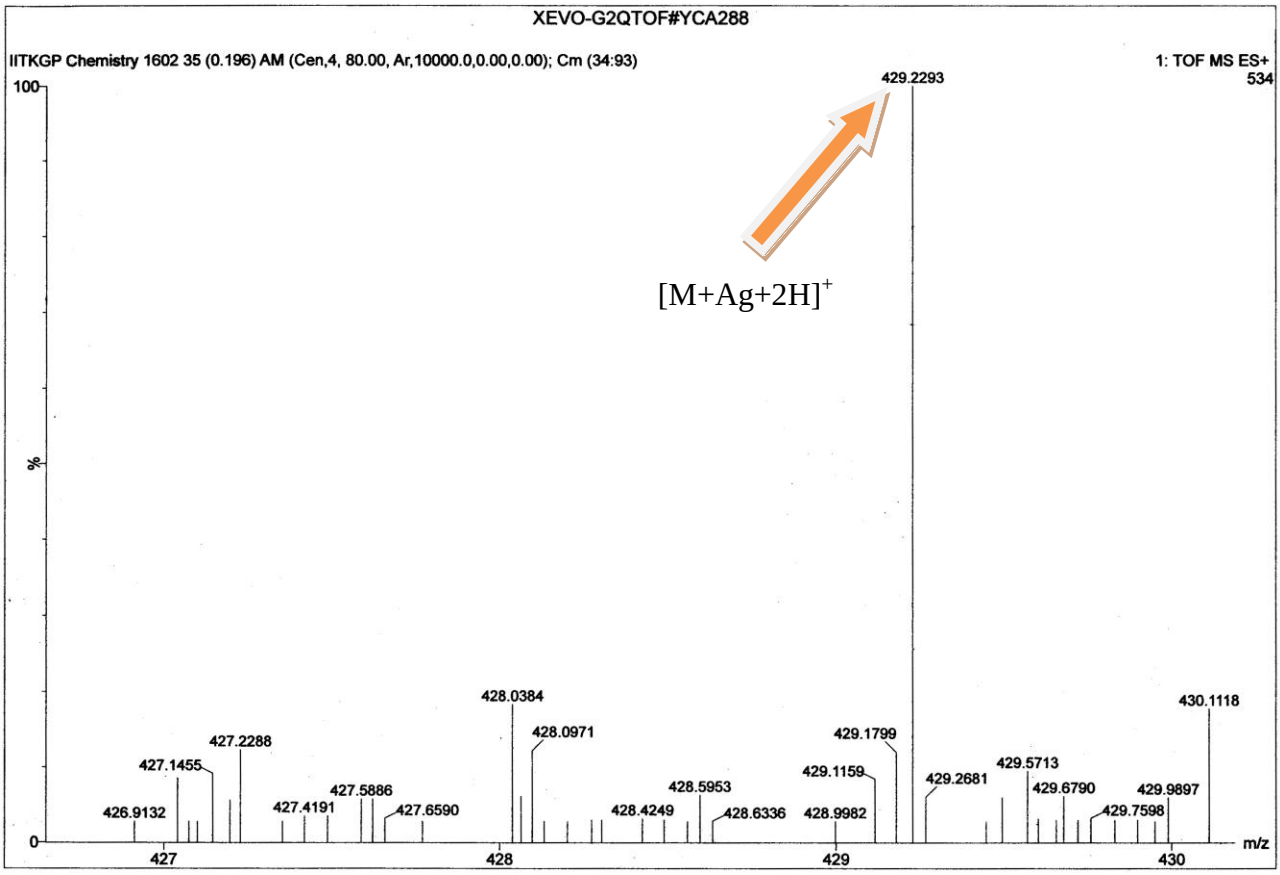

Figure 10A-ESI: HRMS (ESI^+) of a solution of aldehyde **3** with 1 equiv of $AgNO_3$ in H_2O.

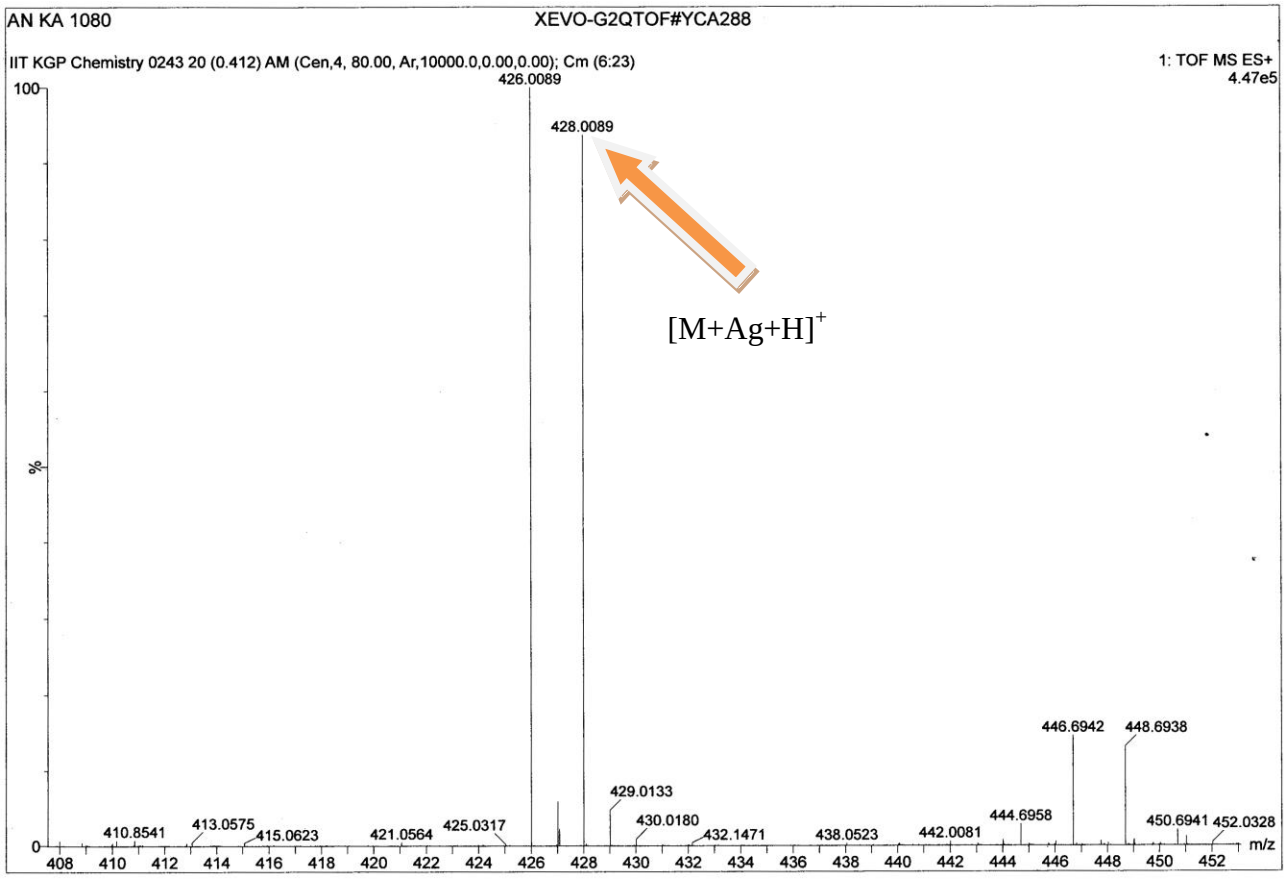

Figure 10B-ESI: HRMS (ESI^+) of a solution of aldehyde **4** with 1 equiv of $AgNO_3$ in H_2O.

AgNPs as antimicrobial agents:

Materials. Bacterial strains *E. coli* and *S. aureus* were used for the antimicrobial studies against the AgNPs. Mueller Hilton broth for antimicrobial studies was obtained from Hi-media.

Method of Antimicrobial assay of AgNPs. Bacterial isolates were inoculated in MHA and incubated at 37 ^{o}C for 12-16 hrs for adequate growth. Isolated colonies from each of the plates were picked up, inoculated in MHB, and incubated overnight in test tubes at 37 ^{o}C. A stock solution of 100 mM silver was prepared. The AgNPs were serially diluted in two stages in a 96-well microtiter plate to a total volume of 290 μL. Then 10μL of overnight culture adjusted to 0.2 McFarland standard was added to the wells and incubated at 37 ^{o}C for 16-18 hrs. The Optical Density was measured at 595nm using multi-plate reader.[5]

Results: The result of antimicrobial activity of the AgNPs has been represented by minimal inhibitory concentration (MIC). This result is shown in table 2-ESI. From this result we observed that our synthesized AgNPs from compound **3** were more effective against Gram-negative organism than Gram-positive ones. This result was compared with the MIC of the AgNPs synthesized from the monosaccharides (glucose and galactose)[6] and disaccharides (maltose and lactose)[6] (Table 3-ESI). From this result we can say that our synthesized AgNPs were more effective against either *E. coli* and *S. aurous* that the AgNPs obtained from glucose, galactose and lactose. Unfortunately the AgNPs obtained from compound **4** did not show any antibacterial activity.

Table 2-ESI: MIC of AgNPs synthesized from **3**

Microbial strains	**MIC (μM)**
E. coli	6.4
S. aureus	12.5

Table 3-ESI: MIC of AgNPs synthesized from naturally occurring mono-and disaccharides.

Microbial strains	**Saccharides**	**MIC (μM)**
E. coli	Glucose	27.0
	Galactose	-
	Maltose	3.38
	Lactose	27.0
S. aureus	Glucose	27.0
	Galactose	54.0
	Maltose	6.75
	Lactose	27.0

References:

1. A. Kayet and T. Pathak, *J. Org. Chem*., 2013, **78**, 9865.

2. B. K. Singh, A. K. Yadav, B. Kumar, A. Gaikwad, S. K. Sinha, V. Chaturvedi and R. P. Tripathy, *Carbohydr. Res*., 2008, **343**, 1153.

3. (a) S. Dey, D. Datta and T. Pathak, *Synlett*., 2011, **17**, 2521; (b) S. Dey and T. Pathak, *RSC Adv*., 2014, **4**, 9275; (c) D. Sahu, S. Dey, T. Pathak and B. Ganguly, *Org. Lett.,* 2014, **16**, 2100.

4. D. Urankar, B. Pinter, A. Pevec, F. De Proft, I. Turel and J. Kosmrlj, *Inorg. Chem.,* 2010, **49**, 4820.

5. S. K. Sarkar, M. Dutta, A. Kumar, D. Mallik and A. S. Ghosh, *PLoS One*, 2012, 7, e48598.

6. A. Panacek, L. Kvitek, R. Prucek, M. Kolar, R. Vecerova, N. Pizurova, V. K. Sharma, T. Nevecna and R. Zboril, *J. Phys. Chem. B,* 2006, **110**, 16248.